

1 **Paleoenvironmental variability and anthropic influence during the last 7,300 years**
2 **in the western Mediterranean based on the pollen record of Cartagena Bay, SE**
3 **Spain**

4

5 María José Gil-García¹, Blanca Ruiz-Zapata¹, José E. Ortiz², Trinidad Torres², Milagros
6 Ros³, Sebastián Ramallo³, Ignacio López-Cilla⁴, Luis A. Galán⁴, Yolanda Sánchez-
7 Palencia², Ignacio Manteca⁵, Tomás Rodríguez-Estrella⁵, Ana Blázquez⁶, Ángeles
8 Gómez-Borrego⁷

9

10 ¹ *Facultad de Ciencias. Universidad de Alcalá de Henares. 28805-Alcalá de Henares.*
11 mjose.gil@uah.es, blanca.ruiz@uah.es.

12 ² *Laboratorio de Estratigrafía Biomolecular. E.T.S.I. Minas y Energía de Madrid,*
13 *Universidad Politécnica de Madrid. C/ Ríos Rosas 21. 28003-Madrid.*
14 joseeugenio.ortiz@upm.es, trinidad.torres@upm.es, yolanda.sanchezpalencia@upm.es.

15 ³ *Departamento de Prehistoria, Arqueología, Historia Antigua, Historia Medieval y*
16 *Ciencias y Técnicas Historiográficas, Universidad de Murcia. C/ Santo Cristo, 1. 30001-*
17 *Murcia.* milaros@um.es, sfra@um.es.

18 ⁴ *Departamento de Infraestructura Geocientífica y Servicios, IGME. C/Ríos Rosas 23.*
19 *28003-Madrid.* i.lopezcilla@gmail.com, l.galan@igme.es.

20 ⁵ *Departamento de Ingeniería Minera, Geológica y Cartográfica, Universidad*
21 *Politécnica de Cartagena. Paseo Alfonso XIII, 52. 30203-Cartagena.*
22 nacho.manteca@upct.es, tomasrestrella@hotmail.com.

23 ⁶ *Instituto Universitario de Medio Ambiente y Ciencias Marinas, Universidad Católica*
24 *de Valencia. C/Guillem de Castro, 94. 46001-Valencia.* ana.m.blazquez@uv.es

25 ⁷ *Instituto Nacional del Carbón (INCAR- CSIC), Apdo. 73, 33080-Oviedo.*
26 *angeles@incar.csic.es.*

27

28 *Corresponding author: joseeugenio.ortiz@upm.es

29

30 **Abstract**

31 In this paper, we conduct a palynological analysis of a high-resolution Holocene record
32 from Cartagena Bay, southeast of the Iberian Peninsula, to establish paleoenvironmental
33 variability of coastal areas in the western Mediterranean region at a centennial-scale over
34 the last 7,300 years. Statistical analysis of four palynozones allows reconstruction of
35 paleotemperature and paleohumidity conditions. *Pinus*, steppic, xerophilous, and
36 Mediterranean taxa persisted continuously through the record, and only during periods of
37 increased humidity did deciduous and Mediterranean taxa expand (Zones II, subzone
38 IIIb). Cooler and dry conditions favored the development of Cupressaceae and scrubs
39 between 7,300 and 7,000 yr cal BP. The mid-Holocene (Northgrippian) mesophytic
40 optimum took place between 6,800 and 4,000 yr cal BP during which time a
41 Mediterranean climate was present and open forest developed, predominantly consisting
42 of Mediterranean taxa and deciduous trees. The gradual rise in aridity in the Meghalayan
43 (4,000-1,700 yr cal BP) led to Mediterranean forest being replaced by steppic and
44 xerophilous vegetation, a change related mostly to a decrease in summer insolation, with
45 superimposed centennial-scale variability in humidity. In parallel with forest degradation
46 caused by increasing aridity, the record shows marked evidence of human influence since
47 4,000 yr cal BP, which accelerated the progression of open landscapes from the
48 Chalcolithic onwards, this change being especially marked during the Roman period.
49 Significant denudation of the landscape can be attributed to the use of fire, as well as due

50 to agriculture and grazing, with a major contributor being intense metallurgical and
51 mining activity in the area. The Cartagena Bay record reported herein shows centennial-
52 scale oscillations in humidity and temperature that correlate with well-known climatic
53 events during the late Holocene in the western Mediterranean region, synchronous with
54 variability in solar and atmospheric dynamics. The alternation of persistent North Atlantic
55 Oscillation modes is likely to have played a key role in regulating humid–arid periods.

56

57 **Keywords:** Pollen analysis, Holocene, aridification, human impact, Western
58 Mediterranean, Cartagena Bay (Spain)

59

60 **1. Introduction**

61 Recent decades have witnessed a diversification of paleoclimatic records, together
62 with the development of reliable dating methods. These advancements have allowed the
63 reconstruction of the main paleoenvironmental changes at different temporal resolutions
64 that have occurred through time.

65 These records and advances in our understanding of the mechanisms that govern
66 climate changes have revealed significant natural variability operating at different time
67 scales in the system (deMenocal, 2000; Mayewski et al., 2004; Crowley and Hyde, 2008;
68 Rodrigo-Gámiz et al., 2011;), such as the orbital (~100,000 yr), suborbital (~10,000 yr)
69 and historical (~1,000-100 yr) (Köhler et al., 2010) scales.

70 The number of well-dated Iberian multiproxy records has increased in recent
71 decades, especially for the Holocene (Carrión et al., 2010) and, to a lesser extent, for the
72 Pleistocene (González-Sampériz et al., 2010). However, Quaternary climatic variability
73 obtained from terrestrial sedimentary sequences continues to be limited. In some
74 exceptional cases, favorable geological conditions have led to the relatively undisturbed

75 accumulation of sedimentary sequences, some of them located in the Mediterranean realm
76 of Europe (Tzedakis, 2007).

77 The analysis of long chronological periods allows inference of the dynamics of
78 ecosystems at different time points, including climatic scenarios similar to current ones,
79 but with distinct features, such as the influence of anthropic activities. In the current
80 scenario of Global Climate Change influenced by human activities (van Kolfshoten et
81 al., 2003), the Mediterranean region is more vulnerable to climate dynamics (Solomon et
82 al., 2007) and should therefore be used as a model system within the geoscientific agenda.

83 Some paleoenvironmental studies in the western Mediterranean realm have
84 detected a millennial- and centennial-scale link between the oscillations of the
85 paleoclimatic proxies of sedimentary records with solar and atmospheric variability (i.e.,
86 North Atlantic Oscillation—NAO) (Di Rita et al., 2018, 2022) and/or ocean dynamics
87 during the Holocene (Moreno et al., 2012; Fletcher et al., 2013; Rodrigo-Gámiz et al.,
88 2014; Ramos-Román et al., 2018a,b). Most terrestrial records in the western
89 Mediterranean region show cyclical changes on a millennial scale. In addition, records of
90 montane and coastal lakes in southern Iberia show climate changes on a centennial scale
91 (Carrión, 2002; Carrión et al., 2007; Martín-Puertas et al., 2008), some of them showing
92 complex relations between rapid climate variability and ecosystem response in Sierra
93 Nevada (García-Alix et al., 2012; Jiménez-Moreno and Anderson, 2012; Ramos-Román
94 et al., 2016, 2018a,b; Mesa-Fernández et al., 2018) and on the southwestern coast of the
95 Iberian Peninsula (Fletcher et al., 2007; Jiménez-Moreno et al., 2015). Therefore, higher
96 resolution studies are needed to analyze the link between solar and atmospheric activity
97 with oceanographic systems and terrestrial environments in this area on shorter time
98 scales (i.e., centennial).

99 Sediments from lakes, peatlands and marine records of the western Mediterranean
100 realm have documented a trend towards aridification during the late Holocene (Jalut et
101 al., 2009; Carrión et al., 2010; Gil-Romera et al., 2010). However, this trend was
102 superimposed by short-term climate variability and human impact, as shown by recent
103 studies in the region (Carrión, 2002; Martín-Puertas et al., 2008; Fletcher et al., 2013;
104 Jiménez-Moreno et al., 2013, 2015; Ramos-Román et al., 2016). The relationship
105 between climate variability, cultural evolution and human impact during the late
106 Holocene has been addressed in some recent paleoenvironmental studies (Carrión et al.,
107 2007, 2010; López-Sáez et al., 2014; Lillios et al., 2016, Ramos-Román et al., 2018a).
108 However, it is still unclear whether climate or human activities have been the main drivers
109 of environmental change (i.e., deforestation) in this area during this period.

110 Furthermore, most of the sequences studied in the western Mediterranean realm
111 are located at high altitude. In this regard, to better understand the paleoenvironmental
112 characteristics of Mediterranean coastal areas during the Northgrippian and Meghalayan,
113 we drilled a new core (E3) in Cartagena Bay. Of note, E3 contains a large, well-preserved
114 record covering the the last 7,300 yr cal BP (11.1 m), thus allowing continuous sampling
115 (with 3 cm intervals) for a high-resolution study. Moreover, intense amino acid
116 racemization and radiocarbon sampling followed by a Bayesian analysis allowed the
117 establishment of a reliable chronology (Ortiz et al., 2021). Therefore, E3 allows
118 observation of plant dynamics over the last 7,300 years, thus making it an exceptional
119 record in the coastal Mediterranean realm.

120 In brief, the palynological study of the coastal record of Cartagena seeks to contribute to
121 a better understanding of 1) the centennial-scale paleoenvironmental variations that
122 occurred in the western Mediterranean realm during the Northgrippian and Meghalayan

123 and to 2) discriminate the anthropic influence on vegetation in the area around the most
124 important city in the region during prehistoric and historical times.

125

126 **2. Geographical setting, climate and vegetation**

127 Located in the southeast of the Iberian Peninsula, Cartagena Bay is an estuarine
128 environment enclosed by craggy sierras (Fig. 1). To the north of the bay, the hills where
129 Punics and Romans built their cities act as a partial lock, separating them from a wide
130 marsh 2 m above the sea level, El Almarjal, which, after intensive drainage, is now
131 covered by buildings.

132 An ephemeral stream, named Benipila Creek, with a catchment area of 72.5 km²
133 (Conesa and García-García, 2003) runs along the southern boundary of El Almarjal marsh
134 debouching at the southern corner of the bay at the “Mar de Mandarache”, where navy
135 facilities were built in the 18th century. El Almarjal marsh received water and sediment
136 from the Benipila, El Hondón and Saladillo Creeks. Other minor streams, which are
137 wadis, built the small alluvial fans of Concepción and Santa Lucia, as well as several
138 minor ones that now reach the bay through the sewage system.

139 This region is characterized by the predominance of a warm and semi-arid ombro
140 climate (*BSh*) or arid warm Mediterranean climate: a subtropical steppe. The region has
141 a mean annual temperature of 20°C and an annual rainfall of 270 mm, with a marked
142 summer drought (Rivas-Martínez and Rivas and Sáenz, 2017).

143

144 *2.1 Present vegetation*

145 The coast of Cartagena is located in the “Murciano-Almeriense” Biogeographic
146 Province, forming part of the Almería Sector, the Eastern Almería Subsector falling
147 within this (Rivas Martínez, 2007). The vegetation in this subsector is composed of shrub
148 formations that include palm hearts (*Chamaerops humilis*), mastic shrubs (*Pistacia*

149 *lentiscus*), wild olive trees (*Olea europaea* var. *sylvestris*), Wisley cream clematis
150 (*Clematis cirrhosa*), and even Cartagena junipers (*Tetraclinis articulata*) in La Unión
151 range (Sánchez Gómez and Guerra Montes, 2003; Nicolás et al., 2004).

152 In the plains, *C. humilis* and black hawthorn (*Rhamnus lycioides*) are dominant,
153 except for the western area in which the jujube (*Zizyphus lotus*) predominates. In the pre-
154 coastal mountain ranges, located in the northern area, *P. lentiscus* is abundant, while in
155 the coastal mountain ranges to the south, the terebinth (*Periploca angustifolia*) is
156 dominant. In the coastal sands, the geosigmatum of saline areas and dunes predominates.

157 Of note, the lower horizon of the thermomediterranean belt, to which Cartagena
158 belongs, is an ecologically unique area that extends from Cabo de Gata to Cartagena,
159 where it is possible to observe North African optimum endemisms such as *T. articulata*,
160 red spike thorn (*Maytenus senegalensis*), rennet (*Withania frutescens*), etc., which grow
161 in cornical formations with *M. senegalensis* subsp. *europaea* (Díez-Garretas et al., 2005)
162 and *P. angustifolia* (*Mayteno-Periploceto* S.).

163 The landscape is a steppe with a predominance of scrub and shrubs. The pre-
164 coastal mountains are wooded, with groves of pine and holm oak, and also mastic and
165 kermes oak bushes. The coastal mountain ranges hold less vegetation, with more trees
166 confined to the shady areas, and the bushes dominating the sunny ones. Coastal salt
167 marshes are covered with meadows of halophilic and hygrophilous plants. This landscape
168 has changed greatly over time. The vegetation cover found by Paleolithic man in this
169 region can be described as a set of thick Mediterranean evergreen bushes, and immense
170 areas of mastic shrubs, in addition to terebinths, Aleppo pines, kermes oak bushes, olive
171 trees, palm hearts, esparto grass, etc. (Carrión et al., 1995; Carrión, 2003) The creeks were
172 occupied by oleanders and reeds. The salt marshes were covered by French tamarisk,

173 salicornia and platebrush, and the coastal sandy areas by Spanish junipers, littoral
174 junipers, and pines.

175 Despite the changes in vegetation that have occurred over time, the coastal
176 mountain ranges of Cartagena, together with the coastal area that extends to the Cabo de
177 Gata (Almería), are home to plant species of enormous scientific and cultural interest.
178 The Iberian and North African plants —present only in this coastal area and in North
179 Africa—stand out above all others, with species as unique as the araar or sictus tree
180 (autochthonous specimens found only in the mountains of Cartagena within all
181 continental Europe), the jujube, terebinth and caralluma plants, among others. Other
182 species present only in the area of Cartagena (endemic) can also be found, such as the
183 Cartagena rockrose (*Cistus heterophyllus* subsp. *carthaginensis*), and others with a
184 distribution restricted to the south-east of the Iberian Peninsula.

185

186 **3. Material and Methods**

187 Core E3 (37°35'59.4"N/ 0°59'15.3"/7 m a.s.l.), reaching ca. 30 m with a diameter
188 of 7 cm, was drilled using a rig with a conventional rotatory drill pipe and direct flow of
189 natural mud. The sediment core was covered with clingfilm and then taken to the
190 laboratory, where it was split in half longitudinally, photographed and stored in a humid
191 chamber until analysis. The core was scraped to remove the most superficial part (ca. 1
192 cm) and thus avoid possible sediment contamination. Two zones were visually
193 distinguished in the stratigraphic record: yellow-brown muds and sands were dominant
194 in the lower part (30–11 m), whereas grayish to black muddy sands predominated in the
195 uppermost 11–3 m, sometimes with clearly recognisable marine plant remains. The
196 uppermost 3 m consisted of a recent infill comprising a mixture of black muds, pottery

197 sherds and broken bricks. We refer to the sampled horizons of the borehole by their depth,
198 in cm, from top to bottom (e.g., level E3-750 is at 750 cm).

199 Chronology between 11.1 m and 3.0 m was obtained through radiocarbon dating
200 (10 samples, Table 1) and amino acid racemization of ostracode valves (30 ostracodes
201 valves from 12 beds, Table 2) (Ortiz et al., 2021). The numerical datings revealed that
202 materials of the upper 11 m belonged to the Middle (8,300-4,200 yr cal BP or
203 Northgrippian) and Upper (> 4,200 yr cal BP Meghalayan) Holocene. A chronological
204 model was constructed for MIS 1 (Ortiz et al., 2021), which was created with the Bayesian
205 R-code package “Bacon 2.3.7” (Blaauw and Christen, 2011), after 9,000 Markov Chain
206 Monte Carlo iterations (Fig. 1 Supplementary Information).

207

208 *3.1 Pollen and Non-Pollen Palynomorphs*

209 A total of 109 samples from core E3 covering the upper 11.1–3.4 m were selected
210 for palynological analysis. Samples were selected at ca. 6 cm intervals, representing 11
211 cm³. Most of the samples showed enough pollen grains, except the interval 10.7–10.2 m
212 and 34 samples that did not reach the minimum required in terms of the number of grains
213 or taxa. In these cases, the pollen content was considered on the basis of presence. The
214 scarcity of pollen in some beds can be explained by diagenetic processes that occurred in
215 some sandy sediments and that may have affected pollen grain conservation. Some sand
216 beds reflect a higher energy environment (fluvial), resulting in less
217 sedimentation/preservation of pollen grains, as well as being an oxidizing medium, thus
218 leading to the destruction of any pollen grains originally present. The extraction of pollen
219 grains followed standardized acid- and alkali-based methods (Coûteaux, 1977; Girard and
220 Renault-Miskovsky, 1969; Goery and Beaulieu, 1979).

221

222 3.2 Screening

223 A total of 43 plant taxa were identified (14 of them were arboreal, 4 bushes, and
224 25 herbaceous), together with 5 aquatic taxa, spores (monoletete and trilete), and 19 Non-
225 Pollen Palynopmophs (NPPs) of diverse affinity (Fig. 2, 3). Pollen data were plotted as
226 the relative frequency of each taxon in the pollen diagram using the TILIA® and TILIA-
227 GRAPH® software package (Grimm, 1987, 2004). There was generally good
228 preservation of pollen content, as reflected by a high abundance of grains, as well as
229 significative taxonomic diversity.

230 Several representative taxa were selected, allowing the discrimination of 14
231 groups on the basis of their environmental significance, some of them formed by a single
232 genus. Apart from aquatic taxa, spores (monoletes and triletes), *Glomus*, *Concentriciste*
233 and 6 NPPs of diverse nature, the main groups were as follows (Table 3): *Pinus*,
234 Cupressaceae, Mediterranean, deciduous, Riparian, Ericaceae, Rosaceae, Cistaceae,
235 *Chamaerops*, steppic, xerophilous, Nitrophilous, *Asphodelus*, and Cosmopolitan plants.

236 In this regard, it should be considered that *Pinus* and Cupressaceae represented,
237 together with deciduous and Mediterranean taxa, regional vegetation, whereas local
238 vegetation was represented by Riparian taxa, Cupressaceae, Ericaceae, Rosaceae,
239 Cistacea and *Chamaerops humilis*. Herbs were grouped considering xerophilous, steppic
240 and Nitrophilous taxa, the remaining herbaceous taxa being included within the group of
241 Cosmopolitan herbs. NPPs from diverse sources were identified, including those of
242 Coprophilous origin, markers of edaphic humidity and fires, and dry, mesoeutrophic, and
243 oligotrophic conditions. *Concentriciste* representatives are linked to erosive processes,
244 and *Glomus* is associated with deforestation processes (Table 3; van Geel, 2001; Carrión
245 and Navarro, 2002; Cugny et al., 2010; Miola, 2012; López-Vila et al., 2014).

246 Thus, taxa were also plotted following their ecological affinities in a synthetic
247 histogram (Fig. 3). The relative percentages of arboreal, shrub and non-arboreal pollen
248 were calculated on the basis of the abundance of pollen grains of the taxa within each
249 group, thus providing a general picture of the relative proportions of Arboreal Pollen –
250 Non- Arboreal Pollen (AP-NAP). However, some samples showed a low pollen content
251 and had no AP vs. NAP representation, and in these cases, we only marked their presence
252 (not the percentage). The percentages of spores and NPPs were calculated separately,
253 based on their abundance, to obtain a consistent picture of the local and regional plant
254 population.

255 To achieve a detailed description of the palynological record, a series of pollen
256 zones were established through a hierarchical cluster analysis with the help of CONISS
257 (Grimm 1987), together with a visual inspection based on changes in the main taxa
258 groups. We also performed a Principal Component Analysis (PCA) on the main groups
259 of pollen assemblages (*Pinus*, Cupressaceae, Mediterranean, deciduous, Cistaceae,
260 xerophilous and steppic taxa) with the software Biplot 1.1 (Smith and Lipkovich, 2002)
261 to clarify the identification of climate oscillations and to visualize the weight the different
262 groups had on the landscape. PCA is a technique used to identify a smaller number of
263 uncorrelated variables known as principal components (PC) from a larger set of data and
264 increasing interpretability. These PCs successively maximize variance. The technique is
265 widely used to emphasize variation and capture strong patterns in a data set. The
266 orthogonal linear transformation that converts the data to a new coordinate system
267 assumes that the directions (axis) with the largest variances are the most “important” (i.e.,
268 the most principal component-PC).

269

270 **4. Results**

271 The most notable observation in the Cartagena record was the predominance of
272 steppic (*Artemisia*, Chenopodiaceae and *Ephedra*) taxa throughout the entire sequence
273 (Figs. 2, 3). However, oscillations in this group, together with the abundance of other
274 taxa, allowed us to describe the paleoenvironmental characteristics interpreted from the
275 palynozones identified in the CONISS cluster analysis (Table 4).

276 From 7,300 to 7,000 yr cal BP (Zone IV), there was a marked predominance of
277 Chenopodiaceae. Also the presence of Cupressaceae, Asteraceae and *Pinus* was
278 remarkable, with other taxa present only in small amounts. In general, there was a
279 progressive development of forest mass (AP) from 7,000 to 4,000 yr cal BP (Zone III),
280 mainly *Pinus*, evergreen *Quercus*, *Olea*, and some deciduous and Riparian
281 representatives such as *Ulmus*, *Alnus*, *Juglans* *Corylus* and deciduous *Quercus*, and
282 Ericaceae, although steppic (Chenopodiaceae and *Ephedra*) and xerophilous taxa were
283 present. It is worth noting the abundance of T-318, and NNP marker of humid conditions.
284 This period was followed by a marked decrease in AP and the rise of herbs, with a sharp
285 increase in *Artemisia* and *Chenopodiaceae*, which ended after 2,000 yr cal BP (Zone II).
286 The pollen record ended (1,850-1,700 yr cal BP) with a sharp decrease in taxonomic
287 biodiversity (Zone I), associated with the loss of tree cover and an overwhelming presence
288 of steppic taxa (Chenopodiaceae and *Artemisia*).

289 These changes were related to relatively significant variations in the development
290 of the pollen groups. The most representative taxa were plotted in the synthetic diagram
291 (Fig. 4). In this study, we used mainly the oscillations of Mediterranean and deciduous
292 taxa, along with steppic, xerophilous and Aquatic taxa, to determine paleoenvironmental
293 and paleoclimatic variability in the study area. Our findings were confirmed by the results
294 of the PCA (see section 4.1). Indeed, the fluctuations in AP, especially the Mediterranean
295 species (e.g., evergreen *Quercus* and *Olea*), have been used previously in other records

296 of the southern area of the Iberian Peninsula (e.g., Sierra Nevada) and the western
297 Mediterranean region as a proxy for paleoclimate changes, with an increase in the
298 development of these taxa generally indicating greater humidity (Fletcher and Sánchez-
299 Goñi, 2008; Jiménez-Moreno and Anderson, 2012; Fletcher et al., 2013, Ramos-Román
300 et al., 2016, 2018a, b; Torres et al., 2020). In contrast, increases in steppic taxa (i.e.,
301 *Chenopodiaceae*, *Artemisia*, *Ephedra*) have been used as an indication of aridity in this
302 area (Carrión et al., 2007; Anderson et al., 2011; Torres et al., 2020).

303

304 **4.1 Principal Component Analysis**

305 PCA provided a scaled pollen index roughly corresponding to paleoclimate
306 variations and this was used to confirm the pollen assemblage zones. The aim was to
307 identify and group samples with similar paleoenvironmental characteristics along the
308 Cartagena record. Thus, we clarified the identification of climate oscillations and
309 visualized the weight that the different pollen groups had on the landscape, as well as the
310 variations they showed.

311 The main results of PCA for the Holocene samples are provided in Table 5. The
312 variables (pollen groups) showed sufficient communality (the proportion of variance of
313 such a variable shared with the others and accounted for by common factors) to validate
314 the results. The scores obtained for PC2 and PC3 were selected for the
315 paleoenvironmental interpretation as they were the ones that better established the
316 clusters which were used to define climatic conditions. In contrast, the scores of PC1 were
317 similar to most of the variables and could not be used to distinguish between paleoclimatic
318 conditions.

319 Thus, the results of the PCA considering PC2 and PC3 were assembled into four
320 main clusters (Fig. 5a). Cluster 1 (C1) was separated with respect to the others because

321 of its positive loading to PC2 and PC3, and it included steppic and xerophilous taxa,
322 whereas Cupressaceae appeared as belonging to C2, characterized by a positive loading
323 to PC2 and negative loading to PC3. C3 comprised *Pinus* and deciduous taxa and was
324 separated due to its negative loading to both PC2 and PC3. Mediterranean taxa and
325 Cistaceae were included in C4 and showed a positive loading to PC3 and negative loading
326 to PC2.

327 PC2 explained 32.2% of the variance. Loadings of PC2 were markedly positive
328 for steppic and xerophilous taxa (C1), typical of arid conditions, while they were negative
329 for Mediterranean and deciduous taxa, typical in wetter environments. PC2 thus appeared
330 to discriminate between herbaceous taxa (*Artemisia*, Chenopodiaceae, *Ephedra*) adapted
331 to low atmospheric moisture (arid to semi-arid conditions), representing open landscapes,
332 and a plant community (Mediterranean and deciduous) requiring adequate rainfall (forest
333 taxa). Thus, PC2 allowed discrimination between open landscapes and forest
334 development.

335 The PCA performed on the pollen dataset showed that 25.4% of the variance was
336 explained by PC3, which was characterized by a positive loading for clusters C1 and C4
337 and a negative loading for clusters C2 and C3. PC3 thus appeared to slightly discriminate
338 between colder (Cupressaceae) and more humid conditions (deciduous). Of note, steppic
339 and Mediterranean taxa showed low positive loadings to PC3, which was interpreted as
340 their presence both in warmer and drier conditions.

341 In this regard, the presence/absence and frequency of *Artemisia* have been
342 traditionally interpreted as the development of cold steppe environments in Europe (Pons
343 and Reille 1988; Follieri et al., 1988; de Beaulie et al., 1992; Reille et al., 2000). However,
344 *Artemisia* was also found in warm/arid conditions in the southern area of the Iberian
345 Peninsula, although at smaller percentages (Díaz de la Guardia and Alba 1998; Ruiz et

346 al., 1999; Sabariego et al., 2002; Torres et al., 2020). Furthermore, the presence of
347 *Artemisia* has been also linked to warm/arid conditions in eastern Iberia during the
348 Holocene (Aranbarri et al., 2014) and the Pleistocene (González-Sampériz et al., 2020).
349 In contrast, the increase in Cupressaceae (*Juniperus*) has traditionally been found to be
350 linked to cold episodes, specially in central and southern Iberian Peninsula (Valdeolmillos
351 et al., 2003; González-Sampériz et al., 2010; Vegas et al., 2010; López-Merino et al.,
352 2012; Iriarte-Chiapusso et al., 2016).

353 Therefore, C1 included steppic and xerophilous taxa, indicating arid scenarios; in
354 C2, Cupressaceae was abundant, linked to colder and semi-arid conditions; in C3,
355 deciduous taxa and Cistaceae were abundant within a warm-temperate/wetter scenario
356 (Mediterranean-like climate with higher moisture); and in C4, Mediterranean taxa
357 predominated in a temperate/wetter scenario (Mediterranean-like climate).

358 To summarize the main characteristics of all the data, we also used a box plot (Fig.
359 6), as it represents the global view of the frequency (qualitative and quantitative) of each
360 variable (group) through the interquartile range and the maximum and minimum values.
361 In brief, the box plot gives information about the distribution and symmetry or asymmetry
362 of the data.

363 Taking these considerations into account, we described the changes in the
364 palynozones in terms of paleoclimatological variations.

365

366 **4.2 Pollen zonation**

367 We identified four pollen assemblage zones (Fig. 4, Table 4), which corresponded
368 to major shifts in Northgrippian and Meghalayan vegetation, these reflecting distinct
369 paleoenvironmental conditions. The pollen concentration was somewhat lower during
370 Zone IV, with an increasing trend in Zone III and Subzone II-d, followed by a decline in

371 Subzone II-c, and high pollen concentrations in Subzones II-b, II-a and Zone I (Fig. 4).

372 The pollen zones are described below:

373

374 **Zone IV** (11.1-10.7 m; 7,300 – 7,000 yr cal BP- Northgrippian)

375 There was reduced tree cover, with the development of Cupressaceae and to a

376 lesser extent *Pinus*, a reduction of Nitrophilic plants (*Plantago* and *Urtica*), the expansion

377 of Cosmopolitan plants and mainly the development of steppic taxa (Chenopodiaceae).

378 In this regard, the Mediterranean forest was represented (evergreen *Quercus*), with slight

379 variations. Of note, palm hearts were present and, overall, drier conditions were detected.

380 Based on the PCA, samples of Zone IV were included in C2 (Fig. 5 a, b). Thus, an open

381 steppe developed, which consisted predominantly of Chenopodiaceae, *Artemisia* and

382 *Ephedra*, linked to greater aridity, together with cooler conditions that would favor the

383 development of Cupressaceae (*Juniperus*) and scrubs. The box plot (Fig. 6) showed high

384 interquartile ranges (47.6-58.1) of steppic plants. Of note, Cupressaceae provided the

385 highest interquartile range in the whole record (9.4-19); their low dispersion and high

386 concentration make these taxa determinant elements in the distribution of the samples in

387 the PCA diagram (C2). Deciduous (1.72) and Mediterranean taxa (2.9) showed low

388 values.

389

390 **Zone III** (10.14–6.54 m; 6,800–4,000 yr cal BP; Northgrippian and Meghalayan)

391 It was characterized by the development of pine forest, the progressive loss of

392 Cupressaceae, and the increase of Mediterranean taxa (evergreen *Quercus* and *Olea*). The

393 presence of Riparian (*Ulmus* and *Alnus*) and deciduous (*Corylus* and deciduous *Quercus*)

394 taxa was relatively constant, while steppic taxa decreased slightly compared to the

395 previous zone, and the presence of xerophilous plants increased. The development of

396 scrubs, mainly Cistaceae, Ericaceae and Rosaceae, together with Cosmopolitan plants,
397 was also constant, while there was a punctual development of Nitrophilous plants
398 (*Plantago*). The differentiation of three subzones was based on the development of the
399 groups considered (Fig. 2-4), as well as on the succession observed in the appearance of
400 the NPP markers of dry conditions (T-3B and T-10) and those associated with wildfires
401 (T-55C and T-7A). NPPs associated with humid conditions (T-315 and T-18) showed
402 their highest content in subzones III-a and III-c,

403 The distribution of samples in the PCA (Fig. 5a, b) followed a dominant pattern,
404 marked by the location of most samples in C3 and C4, defined by the dominance of
405 deciduous and Mediterranean taxa. These observations were reflected in the box plot (Fig.
406 6), characterized by a clear decrease in steppic plants, whose interquartile range (15.1-
407 31.7) explained their small weight in the distribution of the samples in the PCA. The
408 interquartile range (6.5-15.0) of Mediterranean taxa was important for their classification,
409 as was that of *Pinus* (with a range of 16.0-29.0). Another notable observation was the
410 decline of deciduous taxa, whose range varied between 0.5 and 2.57. However, these
411 plants were important for the classification of the samples in the PCA diagram because
412 of the compensated weight of scrub development (Fig. 5a). The position of the samples
413 along each of the clusters (Fig. 5b) revealed the differentiation of the subzones established
414 in the pollen diagram (Fig. 4). Therefore, Subzone III-c (10.2-8.7 m; 6,800-5,650 yr cal
415 BP) was defined by the samples belonging to C3 and C4, with some samples included in
416 C1—dominated by steppic taxa—and C2; samples of Subzone III-b (8.7-7.4 m; 5,650-
417 4,800 yr cal BP) were included in C3, with some also in C4 and C2. Finally, in Subzone
418 III-a (7.4-6.54 m; 4,800-4,000 yr cal BP), the samples were located within C3 and C4.
419 This distribution marked the decline of steppic taxa and the dominance of Mediterranean

420 taxa and scrubs, indicating the development of a Mediterranean climate, with lower
421 humidity than in Subzone III-b and associated with a warmer temperature.

422

423 **Zone II** (648-365 cm; ca. 4,000-1,850 yr cal BP age- Meghalayan)

424 Its main characteristic was the considerable loss of tree cover due to a decrease in
425 pine forest and a less pronounced decrease in other forest taxa. Cupressaceae showed a
426 low and discontinuous presence, steppic (*Artemisia* and Chenopodiaceae) taxa dominated
427 over xerophilous plants, and the presence of Cistaceae and the Cosmopolitan plants were
428 more stable. Aquatic plants appeared with the lowest percentages, as did the NPPs
429 associated with humid conditions (T-315 and T-18), and only a few spores were detected.
430 In contrast, *Glomus* was present. There was a continuous presence of coprophilous NPPs
431 (T-55A, T-113 and T-368), and NPP markers of wildfires (T-55C and T-7A) appeared
432 sporadically. In this framework, the identification of four subzones was defined by the
433 behavior of Steppic taxa, scrubs and Mediterranean taxa (*Olea* and evergreen *Quercus*)
434 (Table 3). Thus, Subzone II-d (6.5-5.7 m; 4,000-3,000 yr cal BP) showed the lowest
435 abundance of the forest taxa and Subzone II-c (5.7-5.3 m; 3000-2800 yr cal BP) low
436 pollen abundance, although the pollen spectrum was similar to that of Subzone IId.
437 Subzone II-b (5.3-4.8 m; 2,800-2,500 yr cal BP) was characterized by the development
438 of a Mediterranean forest (*Olea* and evergreen *Quercus*), an increase in deciduous taxa
439 (*Corylus*), and the decline of xerophilous plants. Subzone II-a (4.8-3.6 m; 2,500-1,850 yr
440 cal BP) was characterized by a considerable increase in steppic taxa (Chenopodiaceae
441 and *Artemisia*), a reduction of the Mediterranean forest and a slight expansion of *Pinus*
442 and Cupressaceae.

443 Samples were located mainly in C1 of the PCA, dominated by steppic taxa, and
444 some were placed in C4, in this case, due to the development of scrub. Thus, the box plot

445 (Fig. 6) reveals the clear dominance of steppic taxa, whose concentration or interquartile
446 range (48.3-66.6) was the highest in the whole record and also presented a symmetrical
447 distribution. It also revealed the low weight of the rest of the pollen groups considered,
448 except for Mediterranean taxa, although this group presented a lower interquartile range
449 than that of the previous zone. The classification samples within the clusters identified in
450 the PCA (Fig. 5a) allowed identification of the subzones defined in the pollen diagram
451 (Fig. 5b), with a dominance of the samples corresponding to Subzones II-d, II-b and II-a
452 in C1, thereby marking an important change in humidity (strong decrease) in the area and,
453 therefore, the type of landscape developed (very open). Only Subzone II-c was distributed
454 between C3 and C4, together with the samples located in the boundary between Subzones
455 II-b and II-a, although in this case they temporarily belonged to C2. All these observations
456 reflect changing conditions in a globally dry context.

457

458 **Zone I** (365-340 cm; 1,850-1,700 yr cal BP- Meghalayan)

459 It was characterized by a sharp decrease in taxonomic biodiversity, associated
460 with the loss of tree cover and an increase in steppic taxa (Chenopodiaceae and
461 *Artemisia*). In the lower part, *Glomus* and coprophilous NPPs showed markedly increases,
462 together with NPPs typical of dry conditions (T-3B) and associated with fire (T7A).
463 Samples of Zone I were located between C4 and C1 in the PCA, following the trend
464 shown in the samples at the top of Zone II, indicating continuity of the processes initiated
465 in it. This observation explained why the box plot (Fig. 6) presented the highest values of
466 steppic taxa and the lowest ones in the rest of the pollen groups.

467

468 **5. Discussion**

469 Here we used pollen analysis to interpret the paleoenvironmental changes that
470 occurred in the sedimentary record of Cartagena Bay during the Northgrippian and
471 Meghalayan. In this study, we used the variations between mainly steppic, Mediterranean
472 and deciduous taxa, together with Riparian and Aquatic taxa, to reconstruct the natural
473 paleoclimatic variability in the southwestern Mediterranean realm since the
474 Northgrippian. Furthermore, we used the development of nitrophilic plant communities,
475 together with some NPPs, to identify anthropic influence.

476 We also compared the pollen record of Cartagena with those of other localities in
477 the Iberian Peninsula (Fig. 7a). It has to be taken in to account that Cartagena is included
478 within a semi-arid climatological region (Rubel and Kottek 2010; Chen and Chen 2013),
479 while Villarquemado (Aranbarri et al., 2014), Navarrés (Carrión and van Geel, 1999) and
480 Siles (Carrión, 2002) belong to the Mediterranean climatic region (Fig. 1). In this regard,
481 the steppic and xerophilous taxa showed a wide predominance along the whole Cartagena
482 record, whereas in the other record did not show such abundance (Fig. 7a). In contrast,
483 the increase in *Pinus* has also been considered a marker of aridity in the other records
484 (Carrión and van Geel, 1999; Carrión, 2002; Aranbarri et al., 2014). Furthermore, these
485 pollen records are located at diverse altitudes, although the general pollen trends showed
486 similar variations.

487

488 *5.1 Thermo-mesophytic Middle Holocene (Northgrippian) optimum*

489 During the Northgrippian, two phases were identified, an initial one (Zone IV)
490 with a marked decline in forest between 11.1 and 10.7 m (ca. 7,300-7,000 yr cal BP). Of
491 note, this event was one of the most significant decreases in Mediterranean and deciduous
492 taxa (up to 5%), paralleled by an increase in Cupressaceae, which would indicate a cold
493 and dry stage as there was also an increase in steppic taxa. This phase may have been due

494 to local altitude and proximity to the sea, although it could also be explained as a response
495 to strong evapotranspiration rates caused by a increase in summer temperatures (Laskar
496 et al., 2004; Fletcher and Sanchez Goñi, 2008; Jiménez-Moreno et al., 2012; Fletcher et
497 al., 2013). These conditions can be correlated with Bond episode 6 (Bond et al., 2001),
498 linked to cold conditions (Fig. 8). In this regard, a high coherence between loss on ignition
499 values in the Burg Lake (Pyrenees) and ice rafted debris (Bond events) has been also
500 observed, which indicates that submillennial climate fluctuations in the Pyrenees can be
501 linked to the North Atlantic influence (Pèlachs et al., 2011).

502 Later (ca. 6,800-4,000 yr cal BP), the pollen diagram showed forest expansion,
503 with the highest values (average 70%) of Mediterranean, deciduous and Riparian taxa
504 (Zone III). This mesophytic optimum supports the notion of wet thermo-mesophytic
505 conditions and forest maximum in the Mediterranean realm during the Northgrippian,
506 which was followed by a progressive rise in aridity and xerophytization between the
507 Northgrippian to Meghalayan. This mesophytic optimum is also detected in continental
508 sequences from the south of the Iberian Peninsula (Figs. 7a, 8), from lowlands (Pantaleón-
509 Cano et al., 1999, 2003; Fletcher et al., 2007) and mountainous areas (van Geel and
510 Carrión, 1999; Carrión, 2002; Carrión et al., 2004, 2007; Jiménez-Moreno and Anderson,
511 2012; Aranbarri et al., 2014; Ramos-Román et al., 2016, 2018 a,b; Mesa-Fernández et al.,
512 2018; Di Rita, 2022), to marine records from the southwestern Mediterranean region
513 (Fletcher and Sánchez-Goñi, 2008; Di Rita et al., 2018, 2022), and in North Africa (Lamb
514 and van der Kaars, 1995) in the period ca. 7,500–4,000 yr cal BP (Figs. 7a, 8). In this
515 regard, Anderson et al. (2011) suggest a certain difference in the age of the mesophytic
516 optimum between montane and subalpine records and coastal ones (Figs. 7a, 8). The
517 forest development and lake water levels could be linked to the different effect of
518 maximum summer insolation and the seasonality of effective rainfall during the

519 Meghalayan. Nevertheless, this optimum lasted until ca. 4,500 yr cal BP in the coastal
520 area of Almería (Pantaleón-Cano et al., 1999, 2003) and in the southern part of the Iberian
521 Peninsula (Gil-Romera et al., 2010), and ca. 4,000 yr cal BP in the coastal area of
522 Mazarrón (Carrión et al., 2018), only 50 km south of Cartagena, and in mountainous sites
523 in this area (Carrión et al., 2004, 2007). Of note, two periods with increasing aridity within
524 the thermo-mesophytic Northgrippian optimum showed a good correspondence with
525 other pollen records (Fig. 7a, Carrión and van Geel, 1999; Carrión, 2002; Aranbarri et al.,
526 2014).

527 Thus, the first phase was linked to humid conditions that can be correlated with
528 data from other records in the western Mediterranean region that also show similar
529 characteristics during Northgrippian and a transition towards drier conditions in the
530 Meghalayan (Carrión and van Geel, 1999; Carrión, 2002; Carrión et al., 2010; Anderson
531 et al., 2011; Fletcher et al., 2013; Aranbarri et al., 2014, among others).

532

533 *5.2 Dry Upper Holocene (Meghalayan)*

534 The pollen record indicated a significant transformation of vegetation during the
535 Meghalayan (ca. 4,000 yr cal BP), with the substitution of Mediterranean and deciduous
536 taxa for steppic and xerophilous species, in parallel with the progression of open
537 landscapes, thereby confirming a progressive tendency towards the aridification detected
538 in the south of the Iberian Peninsula (Fig. 7a). The tendency towards aridification can be
539 clearly seen in Sierra Nevada records, where there was little influence from human
540 activity (Anderson et al., 2011; Jiménez-Moreno and Anderson, 2012; Jiménez-Moreno
541 et al., 2013; Jiménez-Espejo et al., 2014; Ramos-Román et al., 2016, 2018b).

542 This aridification trend that has occurred since the beginning of the Meghalayan
543 is also found in other records of the western Mediterranean realm (Figs. 7a, 8; Lamb and

544 van der Kaars, 1995; Pantaleón-Cano et al., 1999, 2003; van Geel and Carrión, 1999;
545 Carrión, 2002; Fletcher et al., 2007, 2013; Fletcher and Sánchez-Goñi, 2008; Carrión et
546 al., 2010, 2018; Aranbarri et al., 2014). Similarly, there was good correspondence of our
547 findings with general aridification phases inferred from pollen ratios on the
548 Mediterranean coasts of France and Spain (Jalut et al., 2000).

549 This decline in forests in the western Mediterranean region between the
550 Northgrippian and Meghalayan was related to a decrease in winter rains as a consequence
551 of a northward shift of the westerlies (a positive NAO trend), which induced drier
552 conditions in this area (Jiménez-Moreno and Anderson, 2012; Magny et al., 2012;
553 Fletcher et al., 2013; Di Rita et al., 2022). In this regard, the predominant phases of NAO-
554 like circulation (positive and negative) conditioned the climate pattern of the
555 Mediterranean after 6,000 yr cal BP by modulating the long-term trend of intensity and
556 position of the westerlies (Fletcher et al., 2013; Di Rita et al., 2022).

557 In addition, the decrease in summer insolation would have caused progressive
558 cooling, with a reduction in the duration of the growing season, as well as a decrease in
559 the sea surface temperature (Marchal et al., 2002; Fletcher and Sanchez Goñi, 2008),
560 thereby bringing about a decrease in the land-sea contrast, which would be reflected in a
561 reduction of the wind system and a reduced precipitation gradient from sea to coast during
562 the autumn-winter season. Likewise, a climatic transition has been observed in the coastal
563 area of the Apulia region (southern Italian Peninsula (De Santis and Caldara, 2015) at ca.
564 4,500 yr cal BP due to changes in the Mediterranean wind regimes.

565

566 *5.3 Deforestation and anthropic influence*

567 Anthropic impact can be detected on the basis of various palynomorphs. This is
568 the case of nitrophilic plants, such as *Plantago*, Polygonaceae, *Rumex* and *Urtica* (Riera

569 et al., 2004), as well as Chenopodiaceae (Sadori et al., 2013). Some species of
570 Cichorioideae have been described as nitrophilic taxa (Abel-Schaad and López-Sáez,
571 2013) and as indicators of grazing (Mercuri et al., 2006; Florenzano et al., 2015; Sadori
572 et al., 2016). In addition, some NPP groups, such as the coprophiles (*Riccia*, *Sordaria*,
573 *Podospora* and *Sporormiella*) and those linked to fires (*Neurospora* and type T-7A), are
574 also used as indicators of anthropization and land use (van Geel et al., 1989; Riera et al.,
575 2006; Carrión et al., 2007; Ejarque et al., 2015). Following van Geel et al. (1989),
576 Morellón et al. (2016) and Sadori et al. (2016), we also considered soil mycorrhizal fungi,
577 the NPP *Glomus* sp., and *Asphodelus* and *Pseudoeschizaeae circula* (Concentriciste) as
578 indicators of erosive activity. To check anthropic influence we constructed a pollen index
579 that consisted of the sum of Nitrophilous and Coprophilous taxa together with NPPs
580 markers of eutrophication, fire, and erosive processes and these pollen taxa and NPPs
581 taxa (Fig. 7b).

582 We detected evidence of human activity in the area at the top of the sequence (<
583 4,000 yr cal BP). Of note, during the Meghalayan, the pollen indicators of anthropic
584 activities were discrete or sporadic, which would reveal a small amount of anthropic
585 pressure on nearby ecosystems or far extensive activities. In contrast, in the last 4,000 yr
586 cal BP, there were clear signs of the effects of significant anthropic activity on the
587 environment, evidenced by marked deforestation, along with an increase in both
588 Nitrophilic and Coprophilous plant taxa, as well as in NPP markers of eutrophication, fire
589 and erosive processes (Fig. 7b). Thus, human activities drove ecological degradation in
590 the coastal environment of Cartagena and led to a notable reduction of vegetation, with a
591 very clear turning point starting at 4,000 yr cal BP, which was especially marked during
592 the Roman period when maximum degradation occurred. In this regard, in the
593 archeological settlement Punta de Los Gavilanes (50 km from Cartagena), the

594 anthracological sequence highlights extensive deforestation, which has been linked to the
595 local impact of metallurgy since ca. 2,800 yr cal BP (García-Martínez and Ros-Sala,
596 2010; García-Martínez et al., 2013).

597 Thus, the increase in all these taxa points to considerable human intervention on
598 the landscape, which would include the use of fire, agricultural activities, grazing,
599 opening of the landscape, coinciding with the intense mining-metallurgical activity
600 observed in the area of Cartagena since at least ca. 4,500 yr cal BP (Fig. 7b, Manteca et
601 al., 2017; Ortiz et al., 2021, 2022). Moreover, fecal stanols, such as coprostanol and 24-
602 ethylcoprostanol were abundant in the Cartagena record from the late Bronze Age (Fig.
603 7b), thus indicating a continuous presence of human populations and significant pollution
604 input (Ortiz et al., 2022).

605 The changes caused by these activities occurred in a context of great
606 environmental fragility, which may have accelerated their consequences. This intense
607 anthropic activity is also detected in other sequences in the area, such as in the southeast
608 area of the Sierra de las Moreras from the transition from the Final Neolithic to the
609 Chalcolithic (Muñoz Amilibia, 1993; Ros Sala, et al., 2008). Similarly, Carrión et al.
610 (2018) suggested that intense deforestation occurred in the area of Mazarrón after ca.
611 4,000–3,500 yr cal BP and may have begun earlier. Also, in Chalcolithic archaeological
612 sites of Almería, Rodríguez-Ariza (2000) detected significant denudation of the landscape
613 at ca. 4,600-4,300 yr cal BP. In this regard, the south-eastern area of the Iberian Peninsula,
614 especially around Cartagena, is one of the regions in the western Mediterranean realm in
615 which metallurgy first occurred, in particular since ca. 5,100 yr cal BP.

616 Therefore, the significant transformation of vegetation that began ca. 4,000 yr cal
617 BP, with forest degradation and a rise in steppic and xerophytic vegetation caused by
618 increased aridity ran in parallel with human activities, which accelerated the progression

619 of open landscapes from the Chalcolithic onwards, as also observed by Carrión et al.
620 (2007, 2010).

621 Nevertheless, using a high-resolution analysis of fire-vegetation relationships,
622 Gil-Romera et al. (2010) noted that the coastal highlands of southeastern Spain, which
623 were consistently more populated than inland regions, present earlier and more abrupt
624 fire activity, even during the Northgrippian. Indeed, Carrión et al. (2018) detected a
625 burning pattern in palynozone 3 of Mazarrón.

626

627 **6. Conclusions**

628 The pollen analysis of the Cartagena Bay record allowed the paleoclimatic and
629 paleoenvironmental reconstruction of the last 7,300 yr cal BP of the area and the western
630 Mediterranean realm. This study, supported by comparison with other Mediterranean and
631 North Atlantic records, points to a link between vegetation, atmospheric dynamics,
632 insolation, and solar activity during the Holocene.

633 The Northgrippian was characterized by a generalized cold and dry episode at ca.
634 7,300 yr cal BP. A significant optimum was detected between 6,800 and 4,000 yr cal BP,
635 when forest expansion peaked. This occurred as a response to humid winters and very hot
636 and dry summers, as a response to greater seasonality. These interpretations come from
637 pollen data for deciduous, Mediterranean and Riparian taxa. A climatic trend towards
638 aridification occurred during the Meghalayan (ca. 4,000 yr cal BP), which was probably
639 linked to an orbital-scale decreasing trend in summer insolation. This trend was observed
640 in the pollen data, through a strong decrease in arboreal taxa (deciduous, Mediterranean
641 and Riparian), as well as a marked increase in steppic taxa. These events can be correlated
642 with climate variability on a regional and global scale. The cold and arid pulse identified
643 in our study was almost synchronous with the cold events recorded in the North Atlantic

644 and with the decrease in rainfall in the Mediterranean area, probably linked to a
645 persistence of a positive NAO mode.

646 The sharp decrease in Mediterranean, deciduous and Riparian taxa was associated
647 with the development of open landscapes, which points to the installation of more arid
648 conditions. In addition to the natural climate and environmental variability, there was
649 strong evidence of human activities in the area during this period. This observation
650 suggests that the tendency to natural aridification during the Holocene in the southern
651 area of the Iberian Peninsula was intensified by human activities: mainly
652 mining/metallurgical activities, and also open landscapes, agriculture, and grazing. In
653 addition, the analysis carried out in the Cartagena record showed changes in the
654 environment and climate that were almost coincident with the periodicities observed in
655 solar, oceanic and NAO reconstructions and these changes could reflect a close cause and
656 effect relationship between them.

657

658 **Acknowledgments**

659 This paper was made possible by Grant HAR2017-85726-C2-2-P (*Cambios*
660 *ambientales y ocupación humana en el sector central del sureste ibérico*) funded by
661 MCIN/AEI/ 10.13039/501100011033 and by Grant HAR2017-85726-C2-1-P (*Carthago*
662 *Nova desde su entorno litoral: Paleotopografía y evolución medioambiental del Sector*
663 *central del Sureste Ibérico. Dinámica poblacional y productiva*) funded by MCIN/AEI/
664 10.13039/501100011033. We thank two anonymous reviewers for their valuable and
665 helpful comments on the manuscript.

666

667 **References**

668 Abel-Schaad, D., López-Sáez, J.A. 2013. Vegetation changes in relation to fire history
669 and human activities at the Peña Negra mire (Bejar Range, Iberian Central Mountain
670 System, Spain) during the past 4,000 years, *Veg. Hist. Archaeobotany* 22, 199–214.

- 671 Anderson, R.S., Jiménez-Moreno, G., Carrión, J.S., Pérez-Martínez, C., 2011. Postglacial
672 history of alpine vegetation, fire, and climate from Laguna de Río Seco, Sierra Nevada,
673 southern Spain. *Quat. Sci. Rev.* 30, 1615–1629.
- 674 Aranbarri, J., González-Sampériz, P., Valero-Garcés, B.L., Moreno, A., Gil-Romera,
675 G., Sevilla-Callejo, M., García-Prieto, E., Di Rita, F., Mata, M.P., Morellón, M.,
676 Magri, D., Rodríguez-Lázaro, J., Carrión, J.S., 2014. Rapid climatic changes and
677 resilient vegetation during the Lateglacial and Holocene in a continental region of
678 south-western Europe. *Glob. Planet. Change* 114, 50-65.
- 679 de Beaulieu, J.L., Reille, M., 1992. The last climatic cycle at La Grande Pile (Vosges,
680 France). A new pollen profile. *Quat. Sci. Rev.* 11, 431-438.
- 681 Blaauw, M., Christen, J.A., 2011. Flexible paleoclimate age-depth models using an
682 autoregressive gamma process. *Bayesian Anal.* 6, 457-474.
- 683 Bond, G., Kromer, B., Beer, J., Muscheler, R., Evans, M.N., Showers, W., Hoffmann, S.,
684 Lotti-Bond, R., Hajdas, I., Bonani, G., 2001. Persistent solar influence on North
685 Atlantic climate during the Holocene. *Science* 278, 1257-1266.
- 686 Carrión, J.S., 2002. Patterns and processes of Late Quaternary environmental change in
687 a montane region of southwestern Europe, *Quat. Sci. Rev.* 21, 2047–2066.
- 688 Carrión, J.S., Navarro, C., 2002. Cryptogam spores and other non-pollen microfossils as
689 sources of palaeoecological information: case-studies from Spain. *Ann. Bot. Fenn.* 39,
690 1-14.
- 691 Carrión, J.S., Dupré, M., Fumanal, M.P., Montes, R., 1995. A palaeoenvironmental study
692 in Semi-arid Southeastern Spain: the palynological and sedimentological sequence at
693 Perneras Cave (Lorca, Murcia). *J. Archaeol. Sci.* 22, 355-367
- 694 Carrión, J.S., Yll, E.I., Walker, M.J., Legaz, A.J., Chain, C., LÓpez, A., 2003. Glacial
695 refugia of temperate, Mediterranean and Ibero-North African flora in south-eastern
696 Spain: new evidence from cave pollen at two Neanderthal man sites. *Glob. Ecol.*
697 *Biogeogr.* 12, 119-129.
- 698 Carrión, J.S., Willis, K.J., Sánchez Gómez, P., 2004. Holocene forest history of the
699 Eastern plateaux in the Segura Mountains (Murcia, southeastern Spain). *Rev.*
700 *Palaeobot. Palynol.* 132, 219–236.
- 701 Carrión, J. S., Fuentes, N., González-Sampériz, P., Quirante, L. S., Finlayson, J. C.,
702 Fernández, S., Andrade, A. 2007. Holocene environmental change in a montane region
703 of southern Europe with a long history of human settlement. *Quat. Sci. Rev.* 26, 1455–
704 1475.
- 705 Carrión, J. S., Fernández, S., Jiménez-Moreno, G., Fauquette, S., Gil-Romera, G.,
706 González-Sampériz, P., Finlayson, C., 2010. The historical origins of aridity and
707 vegetation degradation in southeastern Spain, *J. Arid Environ.* 74, 731–736.
- 708 Carrión, J.S., Fierro, E., Ros, M., Munuera, M., Fernández, S., Ochando, J., Moreno, A.,
709 2018. Ancient Forests in European drylands: Holocene palaeoecological record of
710 Mazarrón, south-eastern Spain. *Proc. Geol. Associat.* 129, 512-525.
- 711 Chen, D., Chen, H.W., 2013. Using the Köppen classification to quantify climate
712 variation and change: An example for 1901–2010. *Env. Develop.* 6, 69-79.
- 713 Conesa, C., García-García, E., 2003. Las áreas históricas de inundación en Cartagena:
714 problemas de drenaje y actuaciones. *Boletín de la Asociación de Geógrafos Españoles*
715 35, 79-100.
- 716 Coûteaux, M., 1977. A propos de l'interprétation des analyses polliniques de sédiments
717 minéraux principalement archéologiques on le milieu végétal, les faunes et l'homme.
718 In : Laville, H., Renault-Miskovsky, J. (Eds.), *Approche écologique de l'homme*
719 *fossile. Suppl. Bull. Associ. Fran. Etude Quat.* 47, 259-276.

- 720 Cugny, C., Mazier, F., Galop, D., 2010. Modern and fossil non-pollen palynomorphs from
721 the Basque mountains (western Pyrenees, France): the use of coprophilous fungi to
722 reconstruct pastoral activity. *Veg. Hist. Archaeobotany* 19, 391- 408.
- 723 de Santis, V., Caldara, M., 2015. The 5.5-4.5 kyr climatic transition as recorded by the
724 sedimentation pattern of coastal deposits of the Apulia region, southern Italy. *The*
725 *Holocene* 25, 1313-1329.
- 726 deMenocal, P. Ortiz, Guilderson, T., Sarnthein, M., 2000. Coherent High- and Low-
727 Latitude Climate Variability During the Holocene Warm Period. *Science* 288,2198-
728 2202.
- 729 Di Rita, F., Fletcher, W.J., Aranbarri, J. Margaritelli, G., Lirer, F., Magri, D.,
730 2018. Holocene forest dynamics in central and western Mediterranean: periodicity,
731 spatio-temporal patterns and climate influence. *Sci Rep* 8, 8929.
732 <https://doi.org/10.1038/s41598-018-27056-2>
- 733 Di Rita, F., Michelangeli, F., Celant, A., Magri, D., 2022. Sign-switching ecological
734 changes in the Mediterranean Basin at 4.2 ka BP. *Glob. Planet. Change* 208, 103713
735 <https://doi.org/10.1016/j.gloplacha.2021.103713>.
- 736 Díaz de la Guardia, C., Alba, F., 1998. Aerobiología en Andalucía: Estación de Granada
737 (1996-1997). *Red Española de Aerobiología* 3, 21–24.
- 738 Díez-Garretas, B., Asensi, A., Rivas-Martínez, S. 2005. Las comunidades de *Maytenus*
739 *senegalensis* subsp. *Europaeus* (Celastraceae) en la Península Ibérica. *Lazaroa* 26, 83-
740 92.
- 741 Ejarque, A., Anderson, R.S., Simms, A.R., Gentry, B.J., 2015. Prehistoric fires and the
742 shaping of colonial transported landscapes in southern California: A
743 paleoenvironmental study at Dune Pond, Santa Barbara County. *Quat. Sci. Rev.* 112,
744 181– 196.
- 745 Fletcher, W., Boski, T., Moura, D., 2007. Palynological evidence for environmental and
746 climatic change in the lower Guadiana valley (Portugal) during the last 13,000 years.
747 *Holocene* 17, 479–492.
- 748 Fletcher, W.J., Sánchez-Goñi, M.F., 2008. Orbital- and sub-orbital-scale climate impacts
749 on vegetation of the western Mediterranean basin over the last 48,000 yr. *Quat. Res.*
750 70, 451–464.
- 751 Fletcher, W.J., Debret, M., Sánchez-Goñi, M.F. 2013. Mid- Holocene emergence of a
752 low-frequency millennial oscillation in western Mediterranean climate: Implications
753 for past dynamics of the North Atlantic atmospheric westerlies. *Holocene* 23, 153–
754 166.
- 755 Florenzano, A., Marignani, M., Rosati, L., Fascetti, S., Mercuri, A.M., 2015. Are
756 Cichorieae an indicator of open habitats and pastoralism in current and past vegetation
757 studies?. *Plant Biosyst. – Int. J. Deal. Asp. Plant Biol.* 149, 154–165.
- 758 Follieri, M., Magri, D., Sadori, L., 1988. 250,000-year pollen record from Valle di
759 Castiglione (Roma). *Pollen Spores* XXX, 329-356.
- 760 García-Alix, A., Jiménez-Moreno, G., Scott Anderson, R., Jiménez Espejo, F.J., Delgado
761 Huertas, A., 2012. Holocene environmental change in southern Spain deduced from
762 the isotopic record of a high-elevation wetland in Sierra Nevada. *J Paleolimnol* 48,
763 471–84.
- 764 García Martínez, M.S., Ros Sala, M.M., 2010: Gestión del combustible leñoso e impacto
765 medioambiental asociados a la metalurgia protohistórica de Punta de Los Gavilanes
766 (Mazarrón, Murcia). *Trabajos de Prehistoria* 67, 545-559
- 767 García-Martínez, M.S., Grau Almero, E., Ros Sala, M.M., 2013. Woody plants in semi-
768 arid south-eastern Iberia during the Bronze Age: charcoal analysis from Punta de los
769 Gavilanes (Mazarrón, Murcia, Spain). In: Damblon, F. (Ed.), *Proceedings of the*

770 Fourth International Meeting of Anthracology. BAR International Series 2486, pp.
771 103–112.

772 Gil-Romera, G., Carrión, J.S., Pausas, J.G., Sevilla- Callejo, M., Lamb, H.F., Fernández,
773 S., Burjachs, F. 2010. Holocene fire activity and vegetation response in South-Eastern
774 Iberia. *Quat. Sci. Rev.* 29, 1082–1092.

775 Girard, M., Renault-Miskovsky, J., 1969. Nouvelles techniques de préparation en
776 palynologie appliqués à trois sédiments du Quaternaire final de l’Abri Cornille (Istres,
777 Bouches du Rhône). *Bull. del’Assoc. Fran. Etude Quat.* 4, 275-284.

778 González-Sampériz, P., Leroy, S.A.G., Carrión, J.S., Fernández, S., García-Antón, M.,
779 Gil-García, M.J., Uzquiano, P., Valero-Garcés, B., Figueiral, I., 2010. Steppes,
780 savannahs, forests and phytodiversity reservoirs during the Pleistocene in the Iberian
781 Peninsula. *Rev. Palaeobot. Palynol.* 162, 427–457.

782 González-Sampériz, P., Gil-Romera, G., García-Prieto, E., Aranbarri, J., Moreno, A.,
783 Morellón, M., Sevilla-Callejo, M., Leunda, M., Santos, L., Franco-Mugica, F.,
784 Andrade, A., Carrión, J.S., Valero-Garcés, B.L., 2020. Strong continentality and
785 effective moisture drove unforeseen vegetation dynamics since the last interglacial at
786 inland Mediterranean areas: The Villarquemado sequence in NE Iberia. *Quat. Sci. Rev.*
787 242, 106425. <https://doi.org/10.1016/j.quascirev.2020.106425>

788 Goeury, C., De Beaulieu, J.L., 1979. A propos de la concentration du pollen a l’aide de
789 la liqueur de Thoulet dans les sediments minéraux. *Pollen Spores XXI*, 239-251.
790

791 Grimm, E.C. ©., 1987. CONISS: a FORTRAN 77 program for stratigraphically
792 constrained cluster analysis by the method of incremental sum of squares. *Comput.*
793 *Geosci.* 13, 13-35.

794 Grimm, E.C., 2004. TGVView. Springfield: Illinois State Museum Research and Collection
795 Center, Illinois.

796 Jalut, G., Amat, A.E., Bonnet, L., Gauquelin, T., Fontugne, M., 2000. Holocene climatic
797 changes in the Western Mediterranean, from south-east France to south-east Spain.
798 *Palaeogeogr. Palaeoclimatol. Palaeoecol.* 160, 255-290

799 Jalut, G., Dedoubat, J. J., Fontugne, M., Otto, T. 2009. Holocene circum-Mediterranean
800 vegetation changes: Climate forcing and human impact, *Quat. Int.* 200, 4–18.

801 Jiménez-Espejo, F. J., García-Alix, A., Jiménez-Moreno, G., Rodrigo-Gámiz, M.,
802 Anderson, R. S., Rodríguez-Tovar, F. J., Martínez-Ruiz, F., Giralt, S., Delgado
803 Huertas, A., Pardo-Igúzquiza, E. 2014. Saharan aeolian input and effective humidity
804 variations over western Europe during the Holocene from a high altitude record.
805 *Chem. Geol.* 374–375, 1–12.

806 Jiménez-Moreno, G., Anderson, R.S., 2012. Holocene vegetation and climate change
807 recorded in alpine bog sediments from the Borreguiles de la Virgen, Sierra Nevada,
808 southern Spain. *Quat. Res.* 77, 44–53.

809 Jiménez-Moreno, G., García-Alix, A., Hernández-Corbalán, M. D., Anderson, R. S.,
810 Delgado-Huertas, A. 2013. Vegetation, fire, climate and human disturbance history
811 in the southwestern Mediterranean area during the late Holocene, *Quat. Res.* 79, 110–
812 122.

813 Jiménez-Moreno, G., Rodríguez-Ramírez, A., Pérez-Asensio, J.N., Carrión, J.S., López-
814 Sáez, J.A., Villarías-Robles, J.J.R., Celestino-Pérez, S., Cerrillo-Cuenca, E., León,
815 Á., Contreras, C. 2015. Impact of late-Holocene aridification trend, climate
816 variability and geodynamic control on the environment from a coastal area in SW
817 Spain. *Holocene*, 25, 607–617.

818 Köhler, P., Fischer, H., Schimitt, J. 2010. Atmospheric $\delta^{13}\text{CO}_2$ and its relation to $p\text{CO}_2$
819 and deep ocean $\delta^{13}\text{C}$ during the late Pleistocene. *Paleoceanography*, 25, PA1213.

- 820 Iriarte-Chiapusso, M.J., Muñoz-Sobrino, C., Gómez-Orellana, L., Hernández- Beloqui,
821 B., García-Moreiras, I., Fernández-Rodríguez, C., Heiri, O., Lotter, A.F., Ramil- Rego,
822 P., 2016. Reviewing the Lateglacial-Holocene transition in NW Iberia: a
823 palaeoecological approach based on the comparison between disimilar regions. *Quat.*
824 *Int.* 403, 211-236.
- 825 Lamb, H.F., van der Kaars, S., 1995. Vegetational response to Holocene climatic change:
826 pollen and palaeolimnological data from the middle atlas, Morocco. *Holocene* 5, 400–
827 408.
- 828 Laskar, J., Robutel, P., Joutel, F., Gastineau, M., Correia, A.C.M., Levrard, B., 2004. A
829 long-term numerical solution for the insolation quantities of the Earth. *Astron.*
830 *Astrophys.* 428, 261–285.
- 831 Lillios, K.T., Blanco-González, A., Drake, B.L., López-Sáez, J.A., 2016. Mid-late
832 Holocene climate, demography, and cultural dynamics in Iberia: A multi-proxy
833 approach, *Quat. Sci. Rev.* 135, 138–153.
- 834 López-Merino, L., Silva-Sánchez, N., Kaal, J., López-Sáez, J.A., Martínez-Cortizas, A.,
835 2012. Post-disturbance vegetation dynamics during the late Pleistocene and the
836 Holocene: an example from NW Iberia. *Glob. Planet. Chang.* 92-93, 58-70.
- 837 López-Sáez, J.A., Abel-Schaad, D., Pérez-Díaz, S., Blanco- González, A., Alba-Sánchez,
838 F., Dorado, M., Ruiz-Zapata, B., Gil-García, M.J., Gómez-González, C., Franco-
839 Múgica, F., 2014. Vegetation history, climate and human impact in the Spanish Central
840 System over the last 9000 years. *Quat. Int.* 353, 98–122.
- 841 López Sáez, J.A., van Geel, B., Martín, M., 2000. Aplicación de los microfósiles no
842 polínicos en Palinología Arqueológica. In: Oliveira, J.V. (Ed.), *Contributos das*
843 *Ciências e das Tecnologias para a Arqueologia da Península Ibérica. Actas 3º*
844 *Congresso de Arqueologia Peninsular*, vol. IX, Vila-Real, Portugal, Adecap, Porto, pp.
845 11-20.
- 846 López-Vila J, Montoya E, Cañellas-Boltà N, Rull V., 2014. Modern non-pollen
847 palynomorphs sedimentation along an elevational gradient in the south-central
848 Pyrenees (southwestern Europe) as a tool for Holocene paleoecological reconstruction.
849 *The Holocene* 24, 327-345.
- 850 Magny, M., Peyron, O., Sadori, L., Ortu, E., Zanchetta, G., Vannièrè, B., Tinner, W.,
851 2012. Contrasting patterns of precipitation seasonality during the Holocene in the
852 southand north-central Mediterranean, *J. Quat. Sci.*, 27, 290–296.
- 853 Manteca, J.I., Ros, M., Ramallo, S., Navarro, F., Rodríguez-Estrella, T., Cerezo, F., Ortiz,
854 J.E., Torres, T., 2017. Early metal pollution in Southwestern Europe: the former littoral
855 lagoon of el Almarjal (Cartagena mining district S.E. Spain) A sedimentary archive
856 more than 8000 years old. *Env. Sci. Poll. Res.* 24, 10584-10603.
- 857 Marchal, O., Cacho, I., Stocker, T. F., Grimalt, J. O., Calvo, E., Martrat, B., Shackleton,
858 N., Vautravers, M., Cortijo, E., van Kreveld, S., Andersson, C., Koç, N., Chapman,
859 M., Sbaffi, L., Duplessy, J.-C., Sarnthein, M., Turon, J.-L., Duprat, J., Jansen, E., 2002.
860 Apparent long-term cooling of the sea surface in the northeast Atlantic and
861 Mediterranean during the Holocene, *Quat. Sci. Rev.* 21, 455–483.
- 862 Martín-Puertas, C., Valero-Garcés, B.L., Mata, M.P., González- Sampéris, P., Bao, R.,
863 Moreno, A., Stefanova, V., 2008. Arid and humid phases in southern Spain during the
864 last 4000 years: the Zoñar Lake record, Córdoba. *Holocene* 18, 907–921.
- 865 Mayewski, P.A., Rohling, E.E., Stager, J.C., Karlén, W., Maasch, K.A., Meeker, L.D.,
866 Meyerson, E.A., Gasse, F., van Kreveld, S., Holmgren, K., Lee-Thorp, J., Rosqvist,
867 G., Rack, F., Staubwasser, M., Schneider, R.R., Steig, E.J., 2004. Holocene climate
868 variability, *Quat. Res.* 62, 243–255.

- 869 Mercuri, A.M., Accorsi, C.A., Mazzanti, M.B., Bosi, G., Cardarelli, A., Labate, D.,
870 Marchesini, M., Grandi, G.T., 2006. Economy and environment of Bronze Age
871 settlements – Terramaras – on the Po Plain (Northern Italy): first results from the
872 archaeobotanical research at the Terramara di Montale. *Veg. Hist. Archaeobot.* 16, 43.
- 873 Mesa-Fernández, J.M., Jiménez-Moreno, G., Rodrigo-Gámiz, M., García-Alix, A.,
874 Jiménez-Espejo, F.J., Martínez-Ruiz, F., Anderson, R.S., Camuera, J., Ramos-
875 Román, M.J., 2018. Vegetation and geochemical responses to Holocene rapid
876 climate change in the Sierra Nevada (southeastern Iberia): the Laguna Hondera
877 record. *Clim. Past*, 14, 1687–1706.
- 878 Miola, A., 2012. Tools for Non-Pollen Palynomorphs (NPPs) analysis: a list of
879 Quaternary NPP types and reference literature in English language (1972-2011). *Rev.*
880 *Palaeobot. Palynol.* 186, 142-61.
- 881 Mithell, J., 1976. An overview of climatic variability and its causal mechanisms. *Quat.*
882 *Res.* 6, 481-493.
- 883 Morellón, M., Anselmetti, F. S., Ariztegui, D., Brushulli, B., Sinopoli, G., Wagner, B.,
884 Sadori, L., Gilli, A., and Pambuku, A. 2016. Human–climate interactions in the central
885 Mediterranean region during the last millennia: The laminated record of Lake Butrint
886 (Albania). *Spec. Issue Mediterr. Holocene Clim. Environ. Hum. Soc.* 136, 134–152.
- 887 Moreno, A., Pérez, A., Frigola, J., Nieto-Moreno, V., Rodrigo- Gámiz, M., Martrat, B.,
888 González-Sampériz, P., Morellón, M., Martín-Puertas, C., Corella, J.P., Belmonte, Á.,
889 Sancho, C., Cacho, I., Herrera, G., Canals, M., Grimalt, J.O., Jiménez-Espejo, F.,
890 Martínez-Ruiz, F., Vegas-Vilarrúbia, T., Valero-Garcés B.L. 2012. The Medieval
891 Climate Anomaly in the Iberian Peninsula reconstructed from marine and lake records,
892 *Quat. Sci. Rev.* 43, 16–32.
- 893 Muñoz Amilibia, A.M., 1993. Neolítico Final-Calcolítico en el Sureste peninsular: el
894 cabezo del Plomo (Mazarrón-Murcia). *Espacio, Tiempo y Forma, Serie Y, Prehistoria*
895 *y Arqueología*, t. 6. Facultad de Geografía e Historia UNED, Madrid, 133-180.
- 896 Nicolás, M.J., Esteve, M.A., Palazón, J.A., López, J.J., 2004. Modelo sobre las
897 preferencias de hábitat a escala local de *Tetraclinis articulata* (Vahl) Masters en una
898 población del límite septentrional de su área de distribución. *Anales de Biología* 26,
899 157-167
- 900 Ortiz, J.E., Torres, T., López-Cilla, I., Galán, L.A., Sánchez-Palencia, Y., Ros, M.,
901 Manteca, I., Ramallo, S., Navarro, F., Rodríguez-Estrella, T., Blázquez, A., Gómez-
902 Borrego, A., Ruiz- Zapata, B., Gil-García, M.J., Heine, E. 2021. Keys to discern the
903 Phoenician and Roman mining in a typical coastal environment through the
904 multivariate study of trace element distribution. *Sci. Tot. Env.* 790, 1-12.
- 905 Ortiz, J.E., Torres, T., Sánchez-Palencia, Y., Ros, M., Ramallo, S., López-Cilla, I., Galán,
906 L.A., Manteca, I., Rodríguez-Estrella, T., Blázquez, A., Gómez-Borrego, A., Ruiz-
907 Zapata, B., Gil, M.J., 2022. Lipid biomarkers and metal pollution in the Holocene
908 record of Cartagena Bay (SE Spain): Coupled natural and human induced
909 environmental history in Punic and Roman times. *Env. Poll.*
910 <https://doi.org/10.1016/j.envpol.2021.118775>
- 911 Pantaleón-Cano, J., Yll, E.I., Roure, J.M., 1999. Evolución del paisaje vegetal en el
912 sudeste de la Península Ibérica durante el Holoceno a partir del análisis polínico. II
913 Congreso del Neolítico de la Península Ibérica Saguntum-Pla, Extra-2, 17-23.
- 914 Pantaleón-Cano, J., Yll, E.I., Pérez-Obiol, R., Roure, J.M., 2003. Palynological evidence
915 for vegetational history in semi-arid areas of the western Mediterranean (Almería,
916 Spain). *Holocene* 13, 109–119.

- 917 Pèlachs, A., Julià, R., Pérez-Obiol, R., Soriano J.M., Bal, M.C., Cunill, R., Catalán, J.,
918 2011. Potential influence of Bond events on mid-Holocene climate and vegetation in
919 southern Pyrenees as assessed from Burg lake LOI and pollen records. *The Holocene*
920 21, 95–104.
- 921 Perry, C.A., Hsu, K.J., 2000. Geophysical, archaeological and historical evidence support
922 a solar-output model for climate change. *Proc. Natl. Acad. Sci. U. S. Am.* 97, 12433–
923 12438.
- 924 Pons, A., Reille, M., 1988. The Holocene and Upper Pleistocene pollen record from
925 Padul (Granada, Spain): a new study. *Palaeogeogr. Palaeoclimatol. Palaeoecol.* 66,
926 243–263.
- 927 Ramos-Román, M.J., Jiménez-Moreno, G., Anderson, R.S., García-Alix, A., Toney, J.
928 L., Jiménez-Espejo, F.J., Carrión, J.S., 2016. Centennial-scale vegetation and North
929 Atlantic Oscillation changes during the Late Holocene in the southern Iberia. *Quat.*
930 *Sci. Rev.* 143, 84–95.
- 931 Ramos-Román, M.J., Jiménez-Moreno, G., Camuera, J., García-Alix, A., Anderson, R.S.,
932 Jiménez-Espejo, F.J., Carrión, J.S., 2018a. Holocene climate aridification trend and
933 human impact interrupted by millennial- and centennial-scale climate fluctuations
934 from a new sedimentary record from Padul (Sierra Nevada, southern Iberian
935 Peninsula). *Clim. Past* 14, 117–137.
- 936 Ramos-Román, M.J., Jiménez-Moreno, G., Camuera, J., García-Alix, A., Scott Andersen,
937 R., Jiménez-Espejo, F.J., Sachse, D., Ronet, J.L., Carrión, J.S., Webster, C., Yanes Y,
938 2018b. Millennial-scale cyclical environment and climate variability during the
939 Holocene in the western Mediterranean region deduced from a new multiproxy
940 analysis from the Padul record (Sierra Nevada, Spain). *Glob. Planet. Change* 168, 35–
941 53.
- 942 Reille, M., de Beaulieu, J. L., Svobodova, H., Andrieu-Ponel, V., Goeury, C., 2000.
943 Pollen stratigraphy of the five last climatic cycles in a long continental sequence from
944 Velay (Massif Central, France). *J. Quat. Sci.* 15, 665–685.
- 945 Riera, S., Wansard, G., Julià, R., 2004. 2000-year environmental history of a karstic lake
946 in the Mediterranean Pre- Pyrenees: the Estanya lakes (Spain). *Catena* 55, 293–324.
- 947 Riera, S., López-Sáez, J. A., Julià, R., 2006. Lake responses to historical land use changes
948 in northern Spain: The contribution of non-pollen palynomorphs in a multiproxy study.
949 *Rev. Palaeobot. Palynol.* 141, 127–137.
- 950 Rivas-Martínez, S. 2007. Mapa de series, Geoserries y geopermaseries de vegetación de
951 España. *Itinera Geobotanica* 17, 1–436.
- 952 Rivas-Martínez, S., Rivas-Sáenz, S., 2017. Worldwide Bioclimatic Classification
953 System. Available at: <http://www.globalbioclimatics.org/> (accessed 15 June 2017).
- 954 Rodrigo-Gámiz, M., Martínez-Ruiz, F., Jiménez-Espejo, F.J., Gallego-Torres, D., Nieto-
955 Moreno, V., Romero, O., Ariztegui, D., 2011. Impact of climate variability in the
956 western Mediterranean during the last 20,000 years: oceanic and atmospheric re-
957 sponses. *Quat. Sci. Rev.* 30, 2018–2034.
- 958 Rodrigo-Gámiz, M., Martínez-Ruiz, F., Rampen, S.W., Schouten, S., Sinninghe, J.S.
959 2014. Sea surface temperature variations in the western Mediterranean Sea over the
960 last 20 kyr: A dual-organic proxy ($U^{K'}_{37}$ and LDI) approach. *Paleoceanography* 29, 87–
961 98.
- 962 Rodríguez-Ariza, M.O., 2000. El paisaje vegetal de la Depresión de Vera durante la
963 Prehistoria reciente: Una aproximación desde la antracología. *Trabajos de Prehistoria*
964 57, 145–156.
- 965 Ros Sala, M.M., Carrión García, J.S., Navarro Hervás, F., Rodríguez Estrella, T., García
966 Martínez, M.S., Precioso Arévalo, M.L., Portí Durán, M.E., de Miguel Ibáñez, M.P.,

967 Medina Ruiz, A.J., Sánchez González, M.J., Gómez Carrasco, J.G., Atenza Juárez, J.,
 968 Castilla Wandossell, A., 2008 Estudio integral del yacimiento Punta de Los Gavilanes
 969 (Puerto de Mazarrón, Murcia) y su entorno inmediato. Proyecto Gavilanes 2007. XIX
 970 Jornadas de Patrimonio Cultural de la Región de Murcia, Murcia: 57-62
 971 Ruiz, L., Díaz de la Guardia, C., Cano, E., 1999. Aerobiología en Andalucía: estación de
 972 Jaén. *Red Española de Aerobiología* 5, 43–46.
 973 Sabariego, S., Díaz de la Guardia, C., Alba, F., Moa, J.F., 2002. Aerobiología en
 974 Andalucía: estación de Almería. *Red Española de Aerobiología* 7, 33–38.
 975 Sadori, L., Ortu, E., Peyron, O., Zanchetta, G., Vanniére, B., Desmet, M., Magny, M.,
 976 2013. The last 7 millennia of vegetation and climate changes at Lago di Pergusa
 977 (central Sicily, Italy). *Clim. Past*, 9, 1969–1984.
 978 Sadori, L., Giraudi, C., Masi, A., Magny, M., Ortu, E., Zanchetta, G., and Izdebski, A.,
 979 2016. Climate, environment and society in southern Italy during the last 2000 years.
 980 A review of the environmental, historical and archaeological evidence. *Spec. Issue*
 981 *Mediterr. Hol. Clim. Environ. Hum. Soc.* 136, 173–188.
 982 Sánchez Gómez, P., Guerra Montes, J. (2003). *Nueva Flora de Murcia –Plantas*
 983 *Vasculares–*. Ed. Diego Marín, Murcia.
 984 Smith, E. P., Lipkovich, I. A., 2002. Biplot 1.1: Excel Add in freeware. Statistics
 985 Department of Virginia Tech, Blacksburg, VA U.S.A.
 986 <http://www.stat.vt.edu/facstaff/epsmith.htm>
 987 Solomon, S., Qin, D., Manning, M., Marquis, M., Averyt, K., Tignor, M.B., Miller, H.,
 988 Chen, Z., 2007. Contribution of Working Group I to the Fourth Assessment Report of
 989 the Intergovernmental Panel on Climate Change. Cambridge University Press, United
 990 Kingdom-New York.
 991 Rubel, F., Kottek, M., 2010. Observed and projected climate shifts 1901-2100 depicted
 992 by world maps of the Köppen-Geiger climate classification. *Meteorologische*
 993 *Zeitschrift* 19, 135-141.
 994 Torres, T., Valle, M., Ortiz, J.E., Soler, V., Araujo, R., Rivas, M.R., Delgado, A., Julià,
 995 R., Sánchez-Palencia, Y., 2020. 800 ka of palaeoenvironmental changes in the
 996 Southwestern Mediterranean realm. *J. Iberian Geol.* 46, 117-144.
 997 Tzedakis, P.C., 2007. Seven ambiguities in the mediterranean palaeoenvironmental
 998 narrative. *Quat. Sci. Rev.* 26, 2042–2066.
 999 van Geel, B., 2001. Non-pollen palynomorphs. In: Smol, J.P., Birks, H.J.B., Last, W.M.
 1000 (Eds.), *Tracking Environmental Change Using Lake Sediments*, vol. 3. Kluwer,
 1001 Dordrecht, pp. 99-119.
 1002 van Geel, B., Coope, G.R., Van der Hammen, T., 1989. Palaeoecology and stratigraphy
 1003 of the Lateglacial type section at Usselo (The Netherlands). *Rev. Palaeobot. Palynol.*
 1004 60, 25– 129.
 1005 van Kolfshoten, Th., Gibbard, P.L., Knudsen, H.L., 2003. The Eemian Interglacial: a
 1006 Global Perspective. *Introduction. Glob. Planet. Change* 36, 147-149.
 1007 Vegas, J., Ruiz Zapata, M.B., Ortiz, J.E., Galán, L., Torres, T.M García-Cortés, A., Gil-
 1008 García, M.J., Pérez-González, A., Gallardo-Millán, J.L., 2010. Identification of arid
 1009 phases during the last 50 kyr Cal BP from the Fuentillejo maar lacustrine record
 1010 (Campo de Calatrava Volcanic Field, Spain). *J. Quat. Sci.* 25, 1051-1062
 1011 Valdeolmillos, A., Dorado Valiño, M., Ruiz-Zapata, M.B., Bardají, T., Bustamante, I.,
 1012 2003. Paleoclimatic record of the Last Glacial Cycle at Las Tablas de Daimiel National
 1013 Park (Southern Iberian Meseta, Spain). In: Ruiz-Zapata, M.B., Dorado Valiño, M.,
 1014 Valdeolmillos, A., Gil-García, M.J., Bardají, T., Bustamante, I. Martínez Mendizábal,
 1015 I. (Eds.), *Quaternary Climatic Changes and Environmental Crises in the*
 1016 *Mediterranean Region*. Universidad de Alcalá de Henares, pp. 222-228

1017
1018

1019 **Tables**

1020

1021

1022

1023 **Table 1. Radiocarbon age (yr BP) of selected levels from E3 core and calibrated age**

1024 **(cal yr) converted using the Radiocarbon Calibration Program 7.0 (CALIB 7.0)**

1025 **(Stuiver et al., 2014) with the calibration dataset IntCal13 (Reimer et al., 2013)**

1026 **(Ortiz et al., 2021).**

1027

Sample No.	Level (m)	Material	$\delta^{13}\text{C(V-PDB)}$	Conventional age BP	Calibrated BP
CNA5242	3.81	charcoal	-21.3	2,022±28	1,972±76
CNA5243	4.50	charcoal	-23.6	1,955±28	1,907±79
CNA5244	4.83	charcoal	-26.7	2,023±27	1,972±75
CNA5245	5.82	charcoal	-23.0	2,174±28	2,263±45
CNA5246	6.88	Bivalve	2.8	3,817±29	4,219±78
CNA5247	7.41	Bivalve	0.4	4,253±29	4,839±25
CNA5248	8.01	<i>P. oceanica</i>	-11.7	4,731±38	5,455±129
CNA5249	8.07	<i>P. oceanica</i>	-11.2	4,052±36	4,525±103
CNA5250	9.00	<i>P. oceanica</i>	-9.8	3,787±36	4,185±105
CNA5251	10.95	charcoal	-27.4	7,017±46	7,843±103

1028

1029

1030 **Table 2. Mean aspartic acid and glutamic acid racemization ratios obtained in *C.***

1031 ***torosa* valves from E3 core (Ortiz et al., 2021).**

Level (m)	N	D/L Asp	D/L Glu	Age (cal. yr)
3.75	4	0.142±0.001	0.038±0.003	2,639±55
4.65	1	0.146±0.000	0.047±0.000	2,792
4.68	4	0.146±0.003	0.043±0.001	2,789±107
5.16	3	0.146±0.016	0.050±0.012	2,815±671
5.85	4	0.157±0.010	0.051±0.011	3,284±433
6.00	1	0.149±0.000	0.047±0.000	2,916
7.23	2	0.189±0.004	0.052±0.007	4,608±182
8.01	1	0.207±0.000	0.046±0.000	5,372
8.61	1	0.199±0.000	0.048±0.000	5,026
10.05	5	0.252±0.003	0.068±0.002	7,258±145
10.11	2	0.241±0.004	0.062±0.005	6,784±159
10.95	2	0.256±0.026	0.053±0.010	7,413±1073

1032

1033

1034 **Table 3. Main taxa included in the palynological groups identified in the Cartagena record.**

Palynological Groups	Taxa
<i>Pinus</i>	<i>Pinus</i>
Cupressaceae	Cupressaceae
Mediterranean	evergreen <i>Quercus</i> , Oleaceae
Deciduous	<i>Castanea</i> , <i>Corylus</i> , <i>Fagus</i> , <i>Juglans</i> , <i>Tilia</i> , deciduous <i>Quercus</i>
Riparian	<i>Alnus</i> , <i>Betula</i> , <i>Salix</i> and <i>Ulmus</i>
Ericaceae	Ericaceae
Rosaceae	Rosaceae
Cistaceae	Cistaceae
<i>Chamaerops</i>	<i>Chamaerops</i>
Steppic	Chenopodiaceae, <i>Artemisia</i> , Ephedraceae
Xerophilous	Asteraceae liguliflorae (L), Asteraceae tubuliflorae (T), Poaceae
Nitrophilous	<i>Plantago</i> , <i>Polygonaceae</i> , <i>Rumex</i> , <i>Urtica</i>
Cosmopolitan	Rest of herbs
Spores	Monolete and trilete spores
Aquatics	Cyperaceae, <i>Alisma</i> , <i>Epilobium</i> , Ranunculaceae, <i>Typha</i> -m
NPP Coprophilous	<i>Riccia</i> or type 165, <i>Sordaria</i> or type 55, <i>Podospora</i> or type 365, <i>Sporormiella</i> or type 113
NPP edafic humidity	<i>Spyrogira</i> or type 18, <i>Zignema</i> or type 315
NPP dry conditions	<i>Pleospora</i> or type 3B, type 10
NPP mesoeutrophic conditions	<i>Valsaria</i> or type 140, Type 174, Type 181, Type 731
NPP oligotrophic conditions	<i>Rivularia</i> or type 170
NPP fires	<i>Neurospora</i> or type 55C, T-7A
Concentriciste	<i>Asphodelus</i> , <i>Pseudoeschizaeae circula</i>
<i>Glomus</i>	<i>Glomus fasciculatum</i> or type 207

1035

1036

1037 **Table 4.**

1038

Age yr cal BP	Pollen assemblages	Landscape climate
<p>47 taxa (16 arboreal, 4 shrubs, 27 herbaceous). 6 Aquatics, spores (monoletes and triletes) and 19 NPPs of diverse origin. Mediterranean climate with fluctuations in humidity and increase in anthropization</p>		
< 2000	<p>Zone-I Biodiversity decrease. Loss of forest cover. Increase of steppic (Chenopodiaceae). Presence of <i>Glomus</i> and NPP markers of dryness and fire. Lack of Nitrophilous taxa and Coprophilous NPP.</p>	Dry Anthropic
2000 3000	<p>Zone-II Decrease of biodiversity and arboreal taxa. Marked decrease of <i>Pinus</i> and Mediterranean taxa. Sporadic presence of deciduous and Riparian taxa. Absence of <i>Chamaerops</i>. Abundance of steppic (<i>Artemisia</i>, Chenopodiaceae) and xerophilous. Development of <i>Glomus</i> and Coprophilous NPP. Presence of humid NPP, dry NPP and NPP markers of fire.</p> <p>IIa: Development of Cupressaceae. Decrease of Cosmopolitan herbs. Increase of Coprophilous NPP. Presence of NPP markers of fire. IIb: Development of Mediterranean forest (<i>Olea</i>) and decrease of deciduous taxa. Increase of <i>Artemisia</i>. IIc: only presence of Mediterranean taxa, nitrophilous and coprophilous. IId: scarce arboreal cover. Expansion of <i>Artemisia</i>, dry NPP and NPP markers of fire. <i>Pseudoeschizaea</i>.</p>	Dry More anthropic influence
4000 5000 6000	<p>Zone-III Expansion of AP (Mediterranean, <i>Pinus</i>, deciduous and Riparian). Decrease of Cupressaceae. Increase of Aquatics and humid NPP. More diversity of NPP. Punctual presence of <i>Pseudoeschizaea</i> (Concentriciste)</p> <p>IIIa: Maximum of AP (<i>Pinus</i>, evergreen <i>Quercus</i>, <i>Olea</i>, deciduous <i>Quercus</i>, <i>Castanea</i>). Rise of Aquatics and humid NPP. IIIb: increase of <i>Pinus</i> and presence of <i>Corylus</i>, <i>Fagus</i> and <i>Juglans</i>. Low content of xerophilous and steppic. Presence of <i>Chamaerops</i>. Decrease of Aquatics. More dry NPP than humid NPP. <i>Asphodelus</i>. IIIc: progressive decrease of Cupressaceae. Increase of biodiversity and abundance of Mediterranean, deciduous (<i>Corylus</i> y <i>Fagus</i>) and Riparian (<i>Alnus</i>, <i>Salix</i>, <i>Ulmus</i>) taxa, Aquatics and humid NPP. <i>Asphodelus</i> and NPP markers of fire. Low <i>Glomus</i>.</p>	Mediterranean conditions Mediterranean relatively humid
7000	<p>Zone IV Expansion of Cupressaceae. Low <i>Pinus</i> and Mediterranean taxa. Decrease of deciduous, Riparian and Aquatics. Presence of <i>Chamaerops</i>. Abundance of steppic (Chenopodiaceae).</p>	Dry

1039

1040 **Table 5. Principal component (PC) loadings (values higher than 0.5 are marked in**
 1041 **bold), communalities and explained variance in PCA of Holocene sediments.**

1042

Variable	PC 1	PC 2	PC 3	PC 4	Communality
<i>Pinus</i>	-0.723	-0.363	-0.373	-0.234	0.794
Cupressaceae	-0.128	0.595	-0.615	-0.468	0.749
Mediterranean	-0.769	-0.345	0.115	-0.348	0.724
Deciduous	-0.597	-0.148	-0.404	0.725	0.542
Cistaceae	-0.648	-0.095	0.545	-0.135	0.726
Xerophilous	-0.576	0.578	0.086	0.240	0.674
Steppic	-0.354	0.762	0.277	0.036	0.783
% of Variance explained	38.78	27.20	20.40	10.42	

1043

1044

1045 **Figure captions**

1046

1047 **Fig. 1. A)** Geographical location of Cartagena Bay and other records, including the areas
1048 of the Köppen climate classification (Rubel and Kottek 2010; Chen and Chen 2013). 1:
1049 Cartagena; 2: Alborán Sea; 3: Mazarrón; 4: Antas, San Rafael, Roquetas; 5: Siles; 6:
1050 Guadiana; 7: Villaverde; 8: Navarrés; 9: Villarquemado; 10: Tigalmamine; B) Geological
1051 setting of Cartagena with the location of E3 core: (1) El Armarjal marsh; (2) Barrio de la
1052 Concepción alluvial fan; (3) Benipila creek; (4) Navy port, formerly galley port of Mar
1053 de Mandarache; (5) El Hondón creek.

1054

1055

1056 **Fig. 2.** Pollen diagram percentage of the main pollen taxa (Arboreal, Aquatic and NPP)
1057 plotted against depth (m) and age (ka). Pollen assemblage zones (Palynozones), defined
1058 from CONISS cluster analysis are indicated on the right.

1059

1060 **Fig. 3.** Pollen diagram percentage of the main pollen taxa (Shrubs and Herbaceous)
1061 plotted against depth (m) and age (ka). Pollen assemblage zones (Palynozones), defined
1062 from CONISS cluster analysis are indicated on the right.

1063

1064 **Fig. 4.** Pollen diagram inferred from Cartagena record with the percentages of the main
1065 pollen assemblages plotted against depth (m) and age (ka). Pollen assemblage zones
1066 (Palynozones), defined from CONISS cluster analysis are indicated on the right and
1067 described in Table 4. The AP/NAP (Arboreal Pollen/Non Arboreal Pollen) ratio is
1068 included.

1069

1070

1071 **Fig. 5. a)** Principal Component Analysis (PCA) from different pollen taxa showing the
1072 scatter plot with PC2 and PC3 axis; **b)** dowcore plot of the samples identified according
1073 to the clusters differentiated in the PCA.

1074

1075 **Fig. 6.** Box plots showing the frequency values of the main pollen groups (*Pinus*,
1076 Cupressaceae, Mediterranean, deciduous, steppic) in the palynozones.

1077

1078 **Fig. 7. A)** Comparison between the pollen record of Cartagena and that of other Iberian
1079 Peninsula localities: Villarquemado (Aranbarri et al., 2014), Navarrés (Carrión and van
1080 Geel, 1999) and Siles (Carrión, 2002). The location of these sites and the climatological
1081 region to which they belong are shown in Fig. 1. Dark dashed lines represent the Thermo-
1082 mesophytic mid-Holocene (Northgrippian) optimum (TMO) and the Dry Upper Holocene
1083 (Meghalayan) (DUH); and the red dashed lines represent two periods with increasing
1084 dryness. B) Comparison between the sum of pollen grains of Nitrophilic and
1085 Coprophilous taxa, as well as of NPP markers of eutrophication, fire and erosive
1086 processes, with the coprostanol/24-ethylcopostanol index indicative of fecal pollution
1087 (Ortiz et al., 2022) and anthropogenic Pb (Ortiz et al., 2021) along the Cartagena record.

1088

1089 **Fig. 8.** Comparison of paleoenvironmental episodes established for the Holocene in the
1090 Cartagena Basin from the pollen analysis (C) with those of other pollen records from
1091 marine [D: Fletcher and Sánchez-Goñi, (2008); E: Fletcher et al. (2013)]; coastal [F:
1092 Carrión et al. (2018); G: Pantaleón-Cano et al. (1999, 2003); H: Jalut et al. (2000)] and
1093 continental [I: Carrión (2002); J: Fletcher et al. (2007); K: Gil-Romera et al (2010); L:
1094 Lamb and van der Kaars (1995)] records for western Mediterranean. The solar output (A;

1095 Perry and Hsu et al., 1999), and the percentage Drift Ice Index for the North Atlantic
1096 during the last 9 ka BP (B; Bond et al., 2001), are included. IRD, ice rafted debris. Sites
1097 location in Spain are shown in Fig. 1. The two horizontal grey bands marked the
1098 predominance of Mediterranean taxa and thus, thermo-mesophytic conditions.

1099
1100

1101 **Fig. 1 Supplementary Information.** Bayesian age-depth models established for the
1102 Holocene record of E3 core (Ortiz et al., 2021) constructed using the software R-code
1103 package “Bacon 2.3.7”. The black line indicates the single best model based on the
1104 weighted mean age for each depth, and the grey area shows 95% confidence
1105 intervals. Dates were obtained through radiocarbon, and amino acid racemization (Ortiz
1106 et al., 2021; Tables 1 and 2 Supplementary Information).

1107

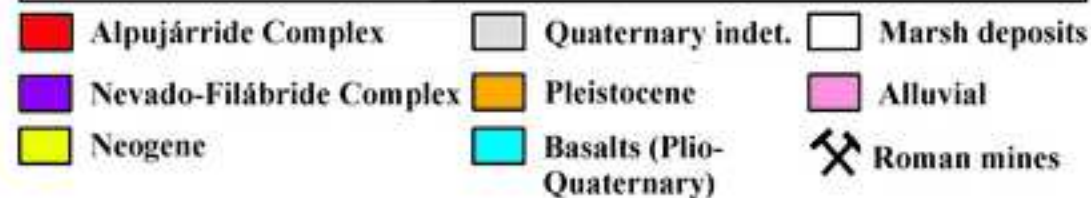
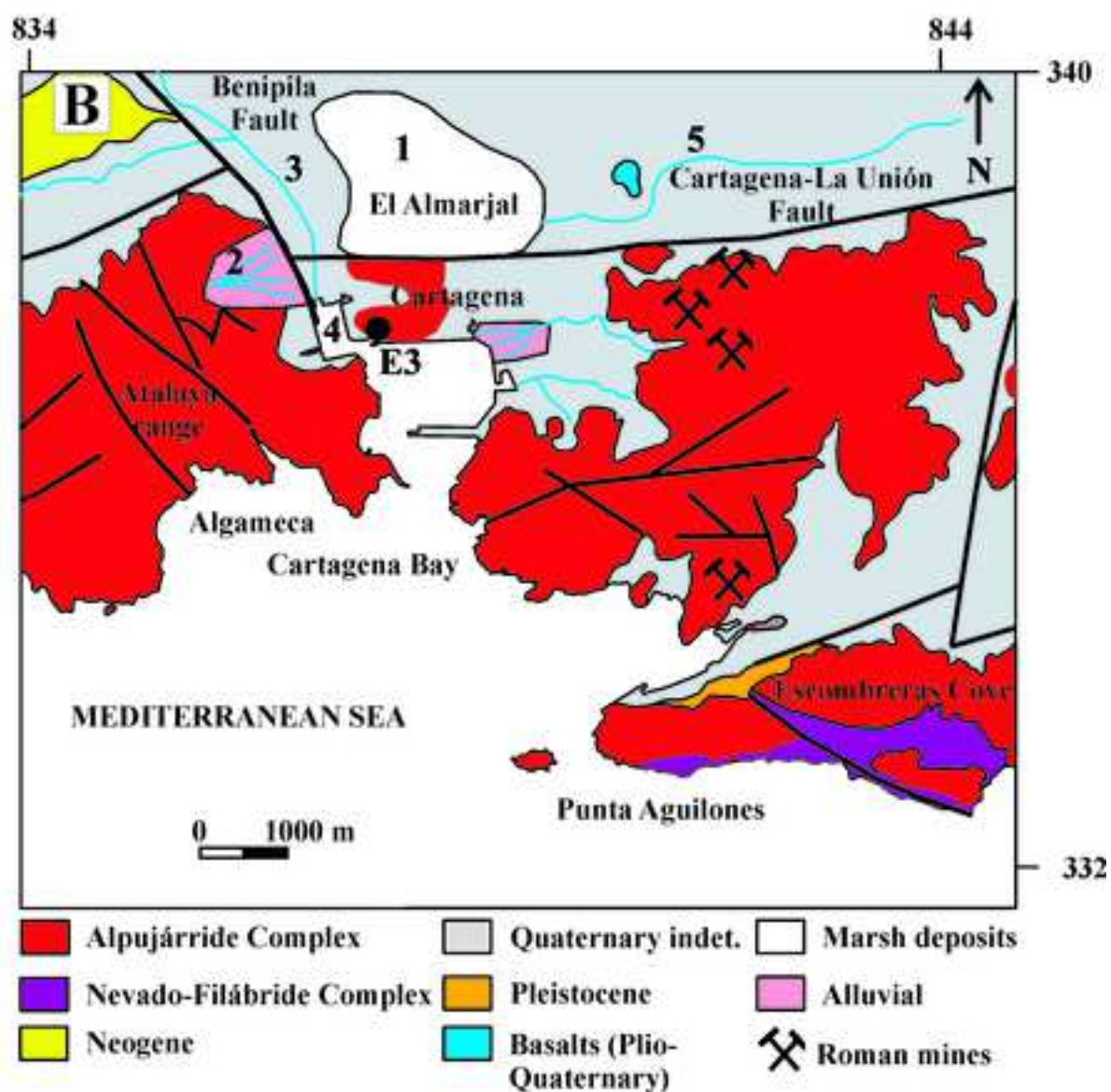
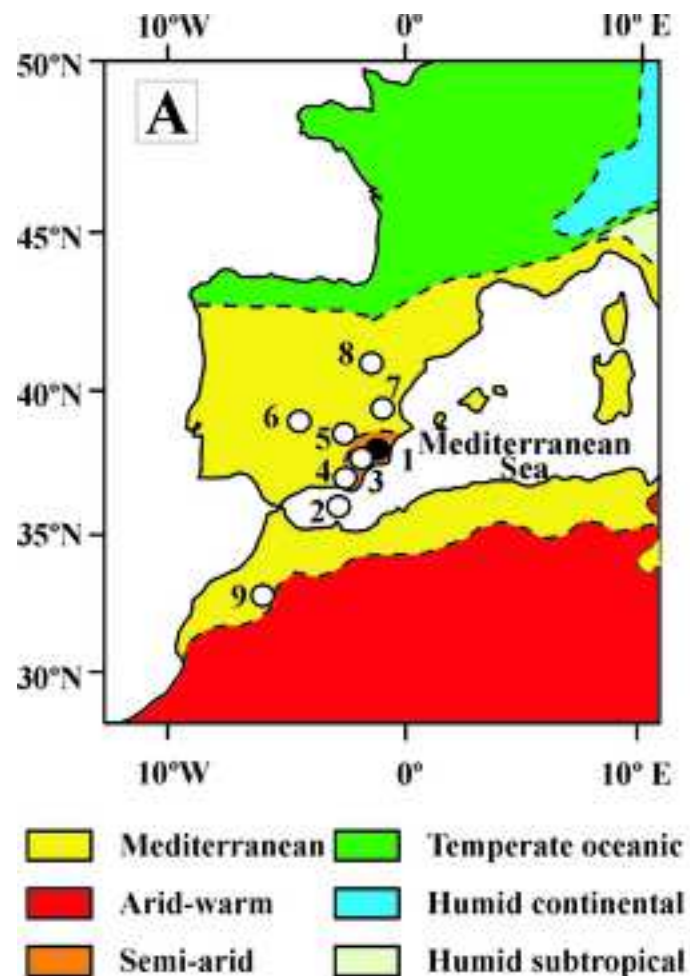


Figure 2

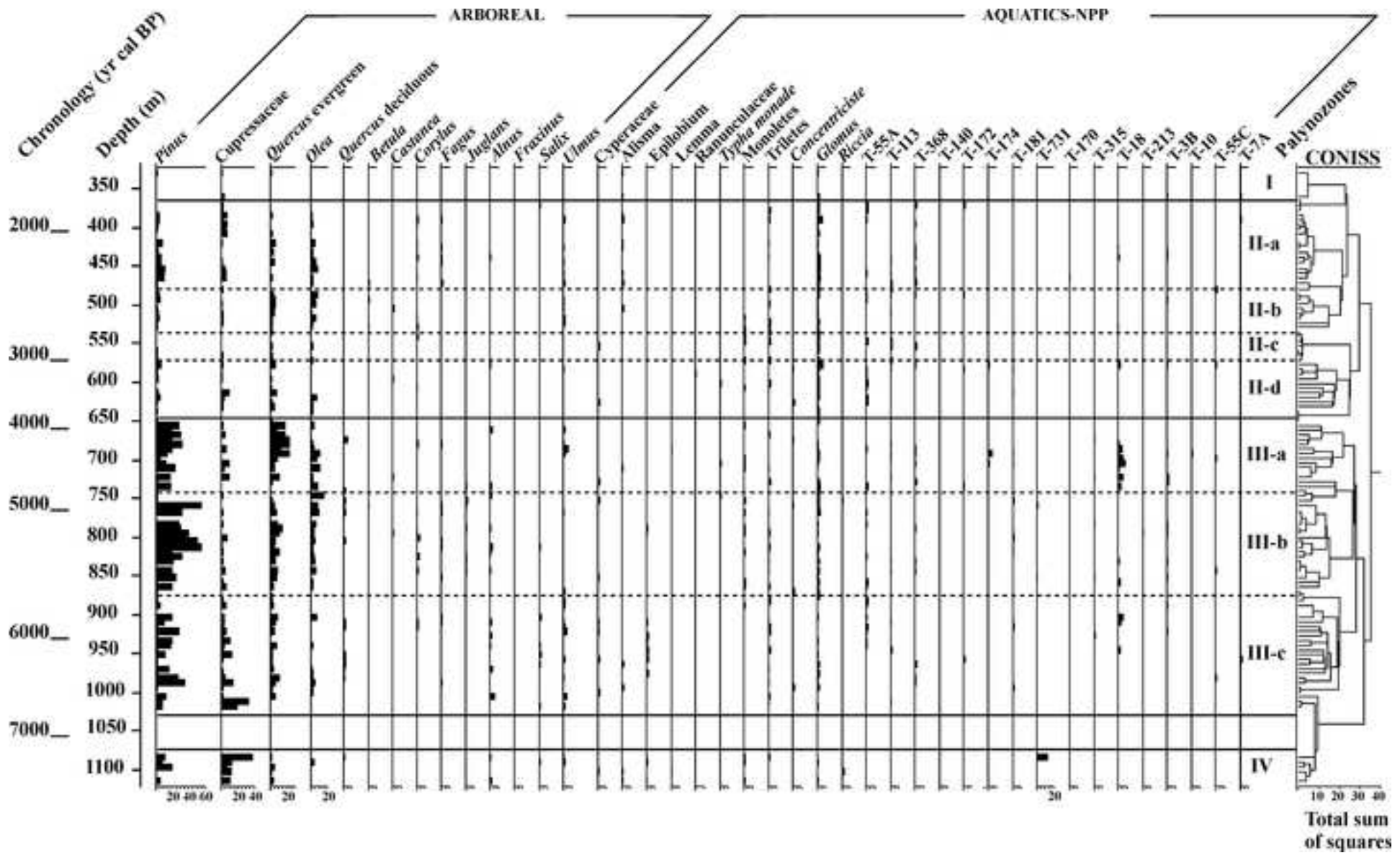


Figure 3

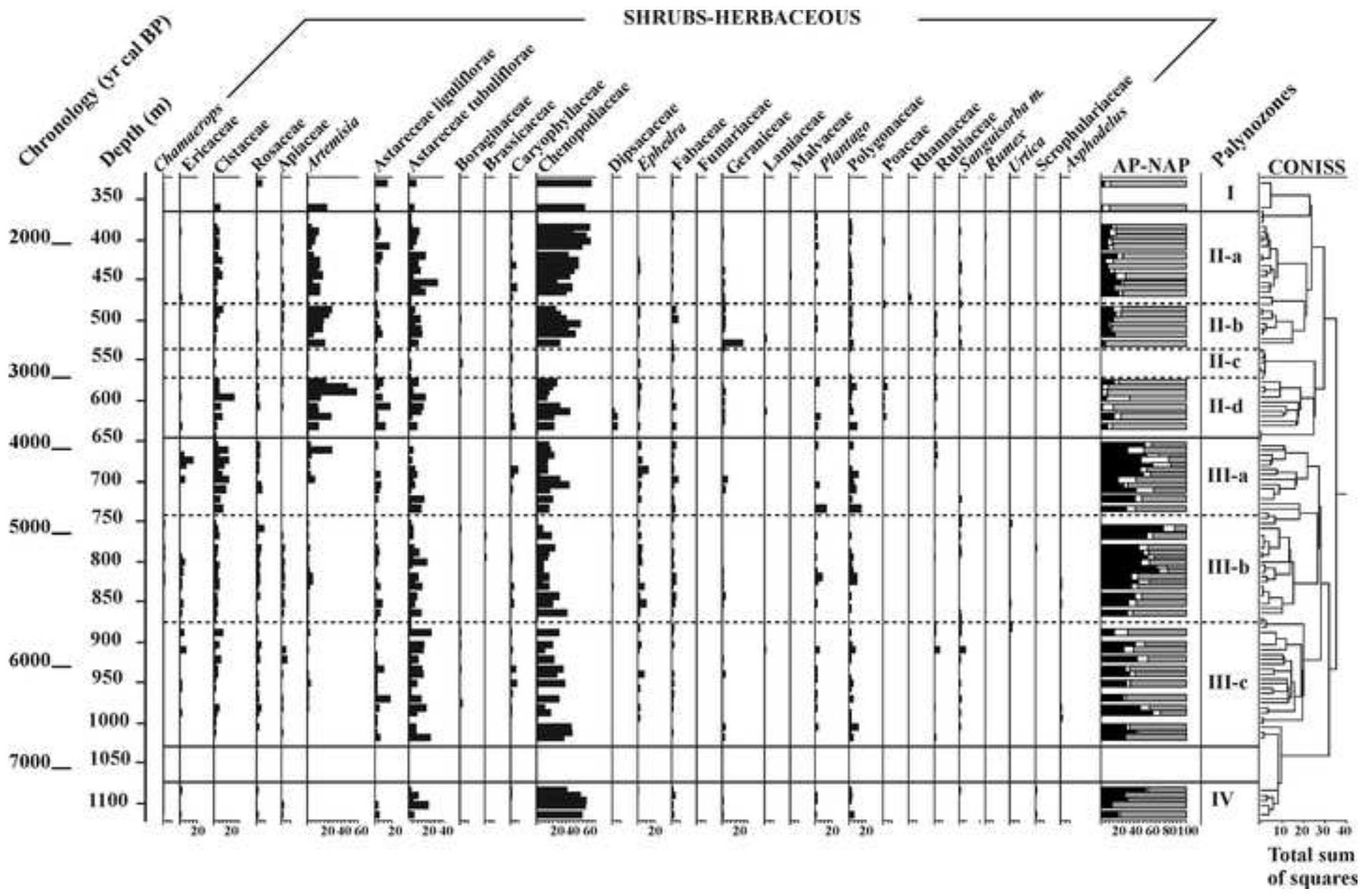
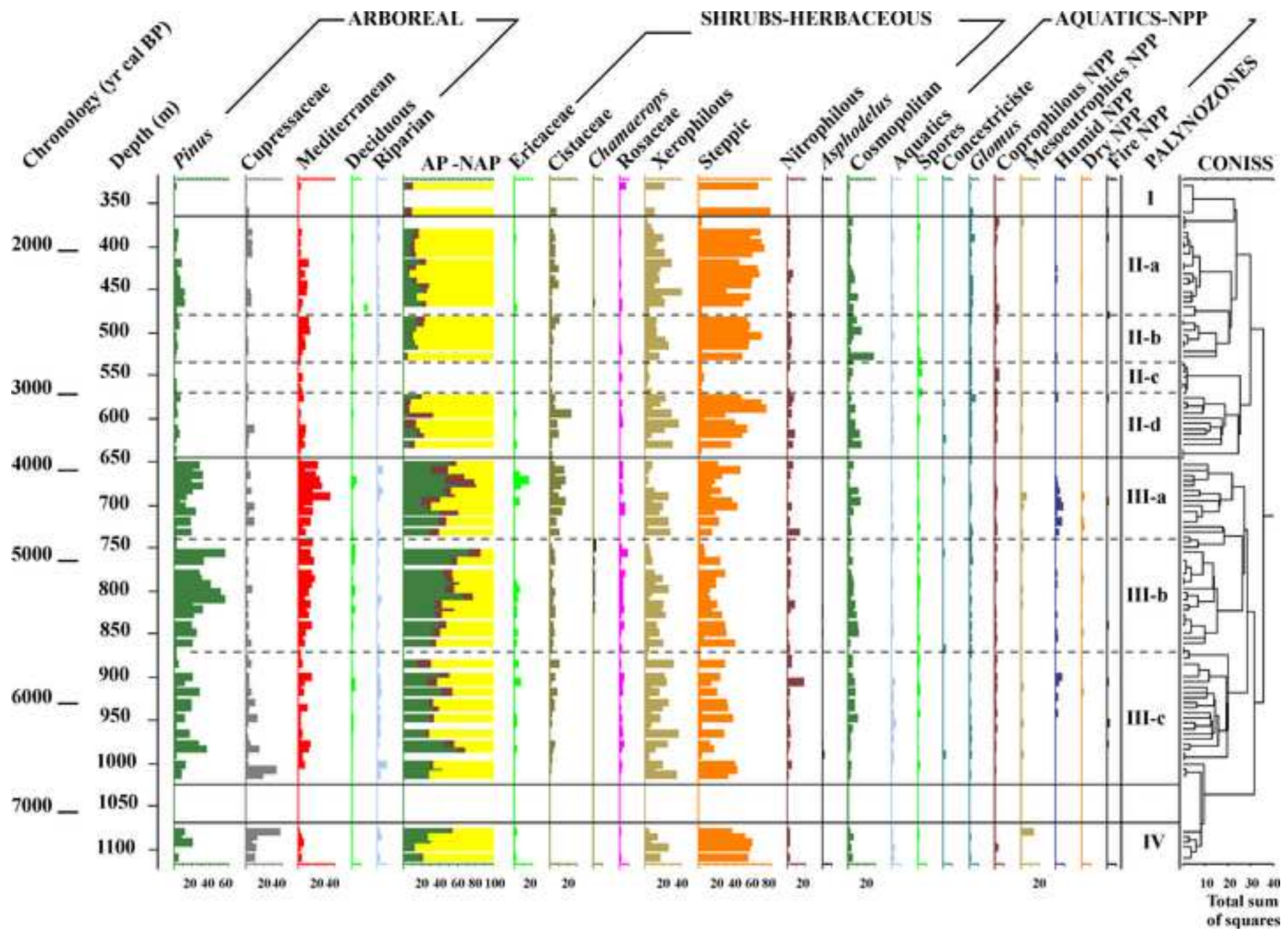
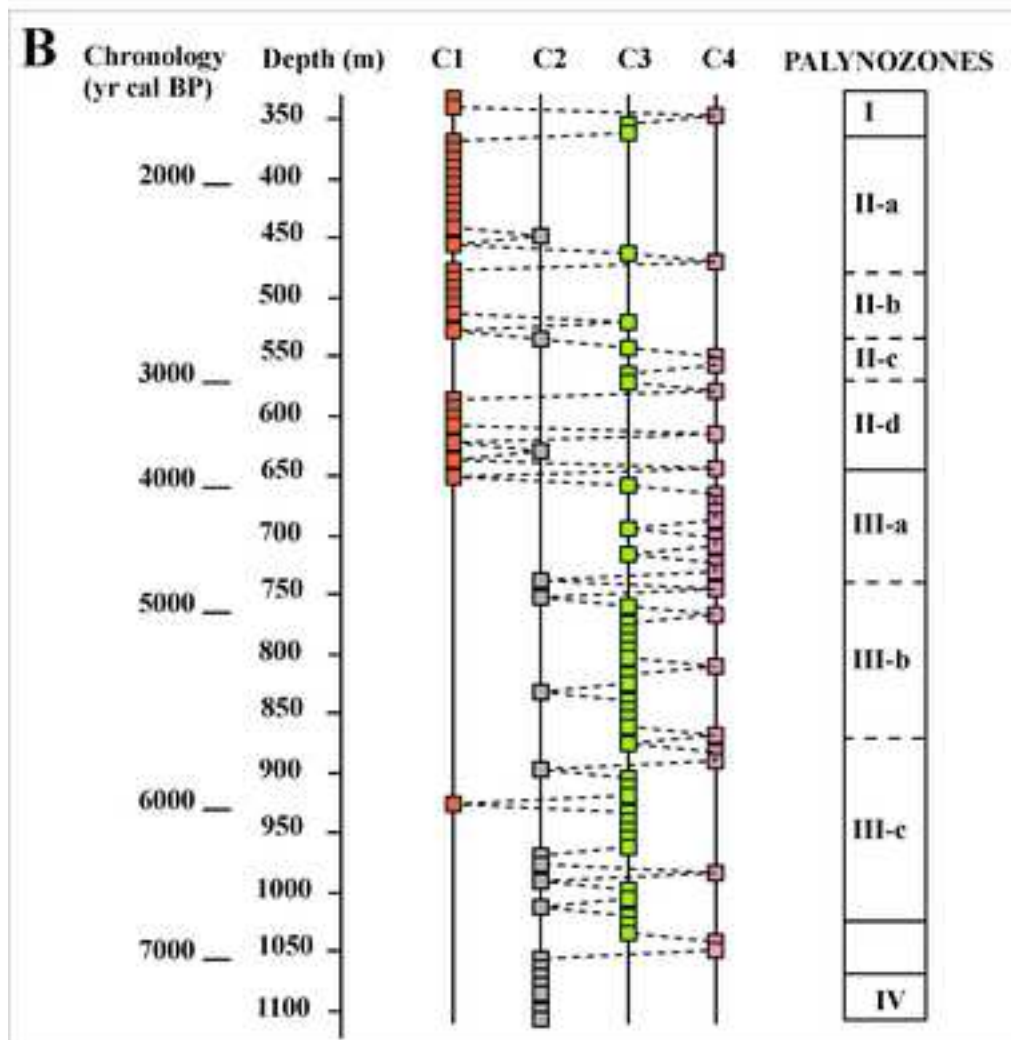
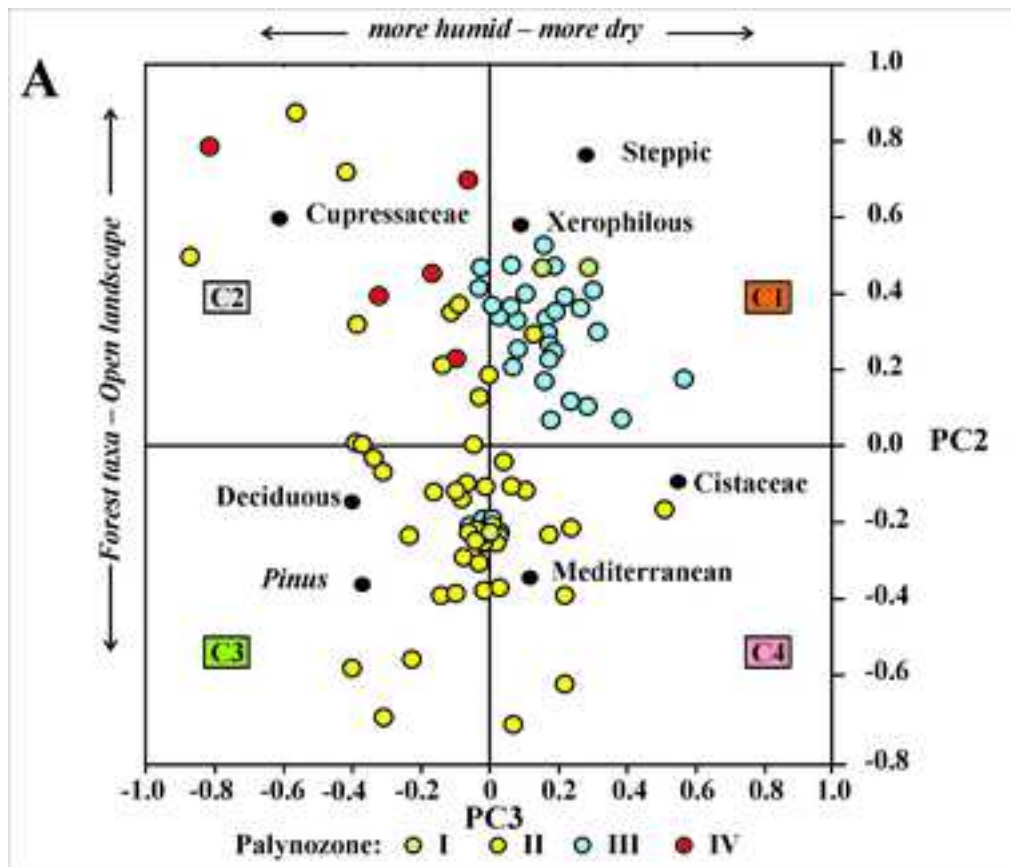
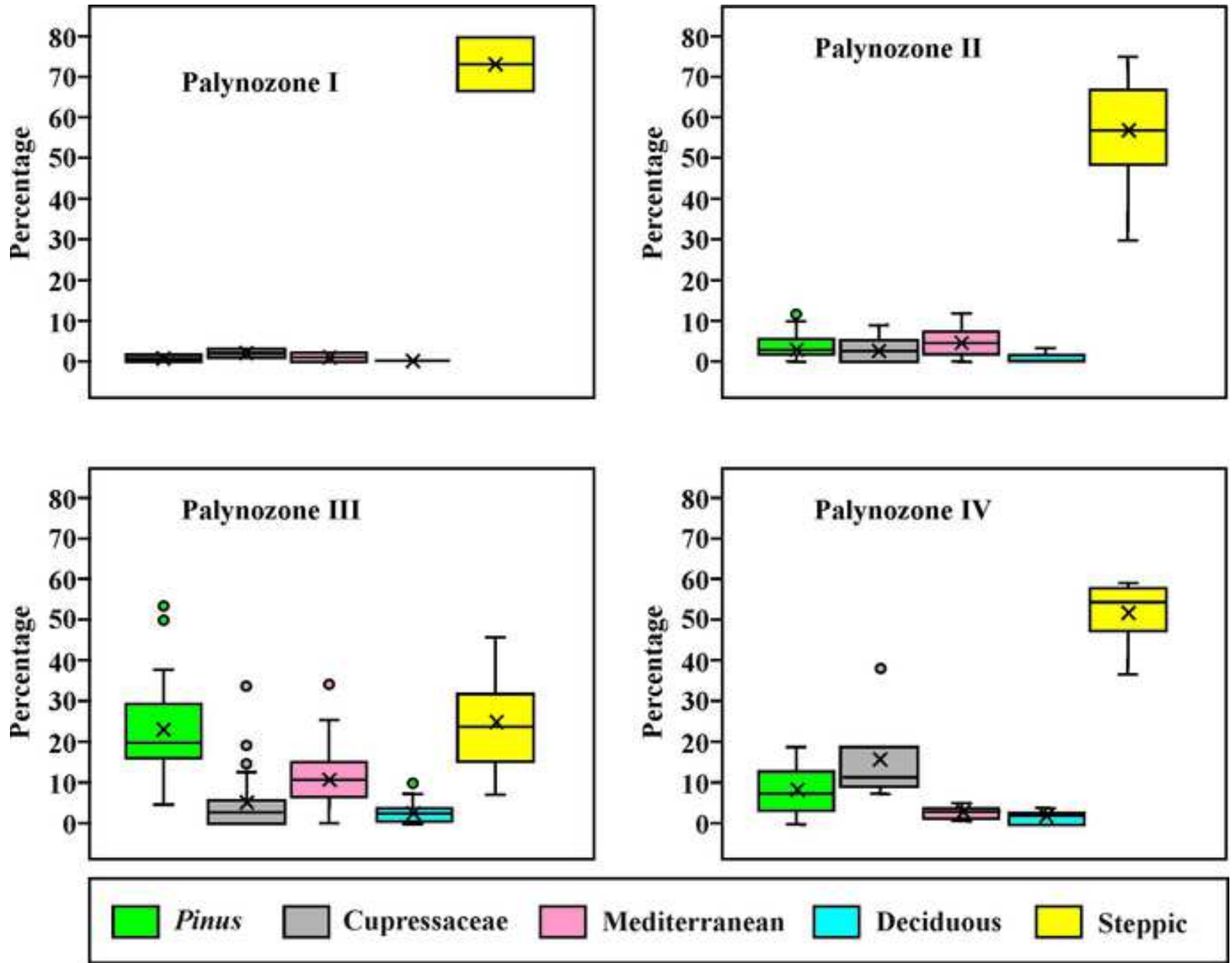
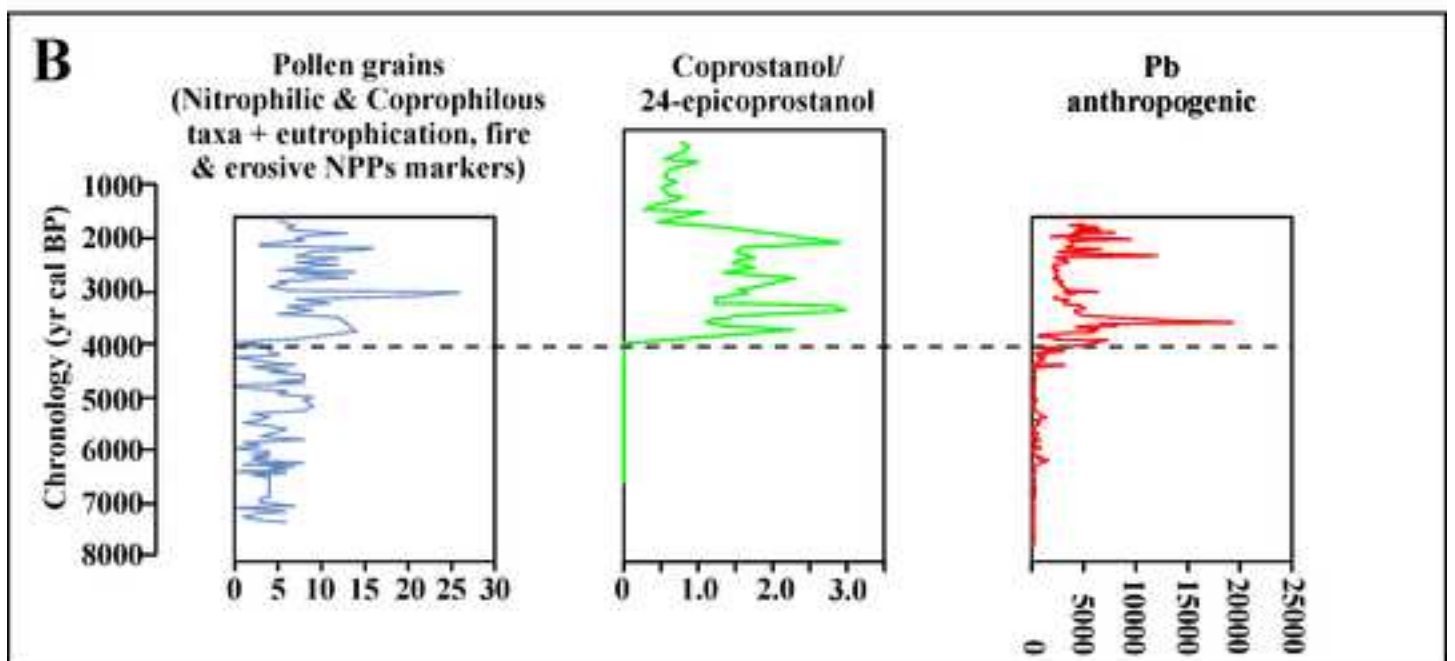
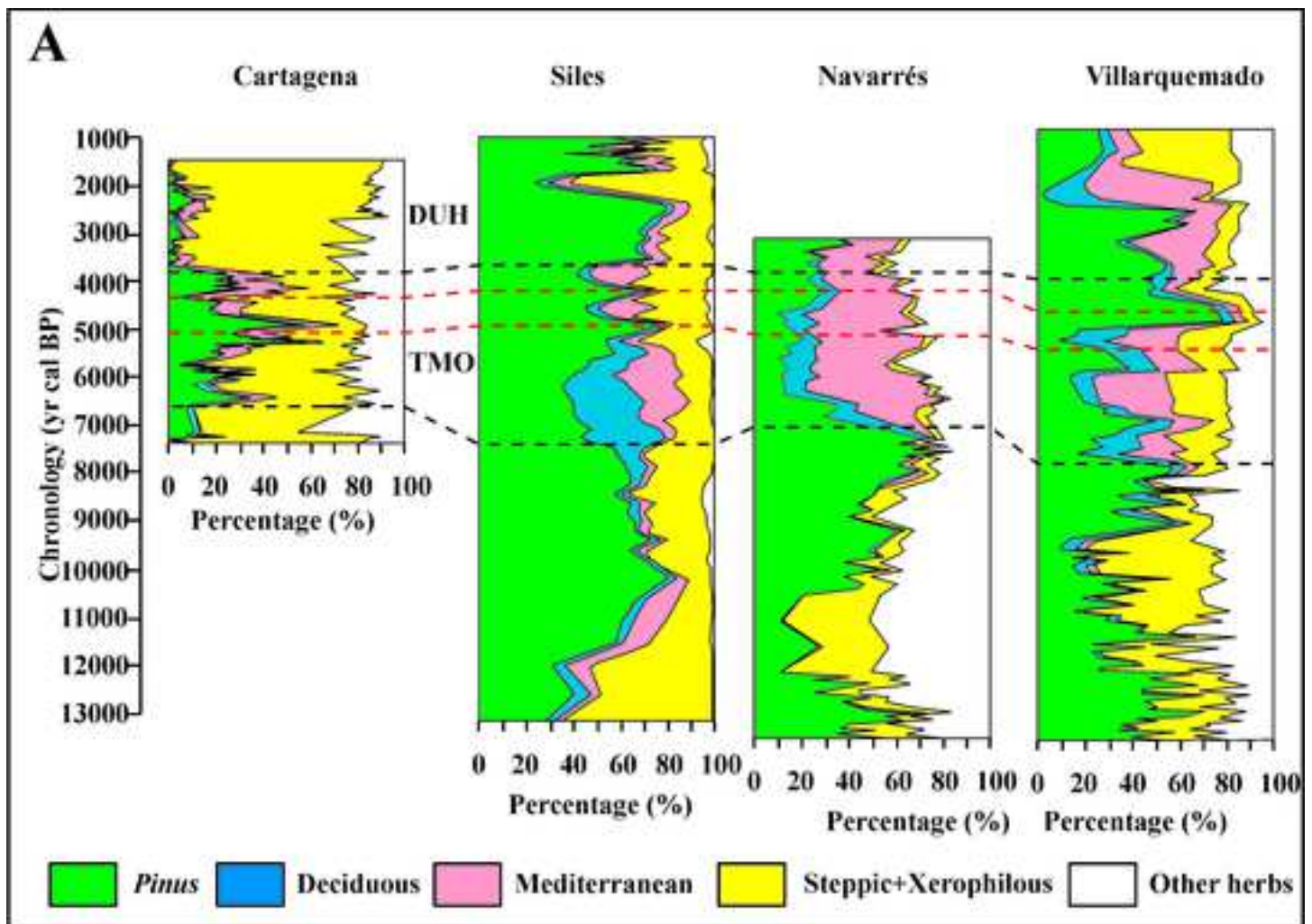


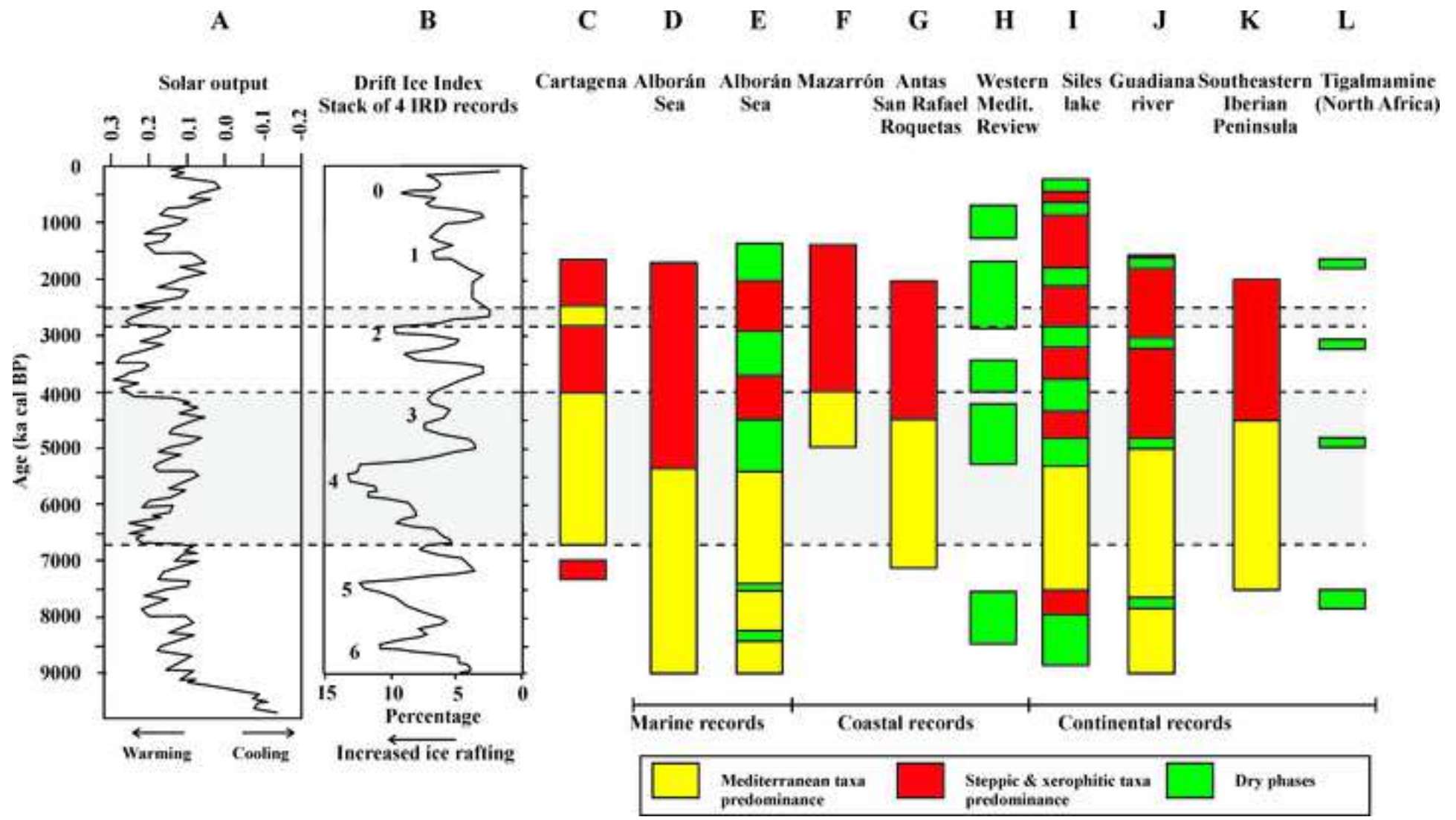
Figure 4











Age (cal yr BP)

MIS 1